421

RECEIVED
APR 11 1994
OSTI

INSTITUTE FOR FUSION STUDIES

DE-FG05-80ET-53088-651 IFSR #651

Solitary Waves and Homoclinic Orbits

N.J. BALMFORTH
Institute for Fusion Studies
The University of Texas at Austin
Austin, Texas 78712

March 1994

THE UNIVERSITY OF TEXAS

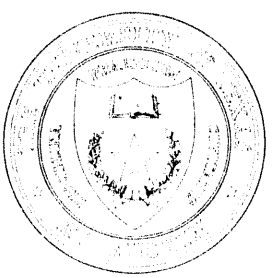

AUSTIN

DISTRIBUTION OF THIS DOCUMENT IS UNLIMITED

Solitary Waves and Homoclinic Orbits

N.J. BALMFORTH
Institute for Fusion Studies
The University of Texas at Austin
Austin, Texas 78712

1 Solitary Waves in Fluids

Ever since Russell's historic observation of a solitary wave in a Scottish canal, the notion that fluid motion often organizes itself into coherent structures has increasingly permeated modern fluid dynamics. Such localized objects appear in laminar flows and persist in turbulent states; from the water on windows on rainy days, to the circulations in planetary atmospheres.

This review concerns solitary waves in fluids. More specifically, it centres around the mathematical description of solitary waves in a single spatial dimension. Moreover, it concentrates on strongly dissipative dynamics, rather than integrable systems like the KdV equation. This divorces it from the theory of solitons, which develops analytically around the inverse scattering transform (*e.g.* Ablowitz and Segur 1981).

One-dimensional solitary waves, or *pulses* and *fronts* (*kinks*) as they are also called, are the simplest kinds of coherent structure (at least from a geometrical point of view). Nevertheless, their dynamics can be rich and complicated. In some circumstances this leads to the formation of spatio-temporal chaos in the systems giving birth to the solitary waves, and understanding that phenomenon is one of the major goals of the theory outlined in this review. Unfortunately, such a goal is far from achieved to date, and we assess its current status and incompleteness.

MASTER

DISTRIBUTION OF THIS DOCUMENT IS UNLIMITED

As experimental analogues of the pulse or frontal dynamics we explore, one can draw on recent experiments with real fluids. Closest to what we describe (in the sense that the equations we use as illustration were once derived as a relevant model) are experiments on falling fluid films. There, as one can often observe on rainy windows and in gutters, waves moving down an incline steepen into propagating pulses (Alekseekno *et al.* 1985, Liu *et al.* 1993). Eventually they are deformed in a second dimension by secondary instabilities, but for a substantial fraction of their evolution, the fluid generates a sequence of essentially one-dimensional pulses, *i.e.* a pulse train. Properties of such patterns of propagating pulses are reviewed by Chang (1994).

Another experimental scenario in which pulses are created involves the convection of a binary fluid, like a mixture of water and ethanol (Anderson and Behringer 1990; Bensimon *et al.* 1990; Moses *et al.* 1987; Niemela *et al.* 1991). When enclosed in a slender geometry like a thin annulus, this fluid can convect heat within localized packets of travelling cells. The manner in which such convective pulses drift, interact and generally evolve provides a powerful visualization of pulse dynamics (Kolodner 1991a, 1991b). Analogous states of excitation exist in liquid crystals (Joets and Ribotta 1988) and in fluids subject to Faraday instability (Wu *et al.* 1984). Various other kinds of solitary waves in interfacial experiments are reviewed by Flesselles *et al.* (1991).

In Sec. 2, we give a brief account of why, theoretically, we might expect many systems to generate solitary waves; we derive the complex Ginzburg-Landau equation for a spatially extended system near a Hopf bifurcation. This suggests that one of the ramifications of overstability is frequently pulse and front generation. It also introduces the notion of spatio-temporal complexity. In Secs. 3 and 4, we turn to the heart of the review; a discussion of the theory of solitary-wave equilibria and dynamics within a framework of asymptotic analysis and dynamical systems theory. In the final section we tie up some loose ends, and briefly mention the standing of the theory with regard to real physical situations.

2 Preliminaries: The Complex Ginzburg-Landau Equation

As a convenient example we take the partial differential equation (PDE),

$$\partial_t u + u\partial_x u + \partial_x{}^2 u + \mu\partial_x{}^3 u + \partial_x{}^4 u + \alpha u = 0 \ , \tag{2.1}$$

where μ and α are parameters. This model equation, for $\alpha = 0$, was derived by Benney (1966) to describe instabilities in falling fluid films; u is the surface displacement about the uniformly thick state. Over a wide range in values of the parameters, this equation possesses solutions that take the form of patterns of pulses (Kawahara and Toh 1987; Elphick *et al.* 1991a; Chang *et al.* 1993a, 1993b).

2.1 Hopf bifurcation in an extended system

The solitary structures observed in systems like binary-fluid convection in annuli occur near the Hopf bifurcation of a spatially extended (one-dimensional) system. In this circumstance, the equations governing the fluid can be asymptotically reduced to a complex Ginzburg-Landau equation governing the spatio-temporal evolution of the envelope of a wave (*e.g.* Manneville 1990). The thin-film Eq. (2.1) admits a spatially uniform equilibrium solution, $u = 0$, which undergoes such a bifurcation when we continuously vary α through positive values. Hence it provides a simple illustration of the derivation of the complex Ginzburg-Landau equation.

The bifurcation to instability occurs as α is decreased through $1/4$. Infinitesimal perturbations about this state have the dependence $\exp[i(kx + \omega t) + \eta t]$, where

$$\omega = \mu k^3 \qquad \text{and} \qquad \eta = 1/4 - \alpha - \left(k^2 - 1/2\right)^2 \ . \tag{2.2}$$

Just below the critical point $\alpha_c = 0.25$, a band of wavenumbers surrounding $k = k_c = 1/\sqrt{2}$ become marginally unstable. Here, we set $\alpha = 0.25 - \varepsilon^2\alpha_2$, where ε is a small parameter

(quantifying "just below") and α_2 is order unity. Near the maximally unstable wavenumber, k_c, the dispersion relation reduces to

$$\omega \simeq \omega_c + \frac{3}{2}\varepsilon\mu K \qquad \text{and} \qquad \eta \simeq \varepsilon^2(\alpha_2 - K^2) \ , \tag{2.3}$$

where $\omega_c = \mu/2\sqrt{2}$ is the corresponding frequency and $k - k_c = \varepsilon K$.

In a spatially extended domain, we see that a packet of linearly unstable waves develops through instability over a distance of order ε^{-1}, and on a timescale of order ε^{-2}. Frequency corrections occur on the shorter timescale ε^{-1}, however, and their dependence on K implies a drift in the envelope of the wave pattern, or a group velocity, εc_g, with $c_g = 3\mu/2$. This observation motivates our asymptotic scaling of Eq. (2.1) in developing a weakly nonlinear theory for the evolution of the envelope of a wave pattern at finite amplitude. In particular, we seek a solution,

$$u \sim \varepsilon \left[A(\varepsilon x, \varepsilon t, \varepsilon^2 t)\, e^{i(k_c x + \omega_c t)} + A^*(\varepsilon x, \varepsilon t, \varepsilon^2 t)\, e^{-i(k_c x + \omega_c t)} \right] \ , \tag{2.4}$$

where $*$ means complex conjugate, and the amplitude $A(\varepsilon x, \varepsilon t, \varepsilon^2 t)$ describes the modulation of the wave pattern.

We now introduce the stretched timescales, $\tau = \varepsilon t$ and $T = \varepsilon^2 t$, and the long length scale, $X = \varepsilon x$, so the temporal and spatial derivatives become,$\partial_t \to \partial_t + \varepsilon\partial_\tau + \varepsilon^2\partial_T$ and $\partial_x \to \partial_x + \varepsilon\partial_X$. We further pose the asymptotic expansion,

$$u = \varepsilon u_1 + \varepsilon^2 u_2 + \varepsilon^3 u_3 + \ldots \tag{2.5}$$

of which the first term is given by the right-hand side of Eq. (2.4). At subsequent orders we derive equations for u_2, u_3 and so on. As is typical in asymptotic expansions of this kind (Manneville 1990), these relation take the form of inhomogeneous linear equations. Requiring the corrections to be bounded enforces certain solvability conditions. In the example at hand, the first condition is

$$\partial_\tau A + c_g \partial_X A = 0 \ , \tag{2.6}$$

which has solution $A = A(X - c_g\tau, T)$; as advertised, the envelope of the wave pattern moves with the group velocity c_g. A modulation equation for A actually emerges from solvability at order ε^3. It is,

$$\partial_T A = \alpha_2 A + (4 - 3i\mu\sqrt{2})\partial_X{}^2 A - \frac{(10 + 7i\mu\sqrt{2})}{(50 + 49\mu^2)} |A|^2 A \ , \tag{2.7}$$

which is a particular case of the complex Ginzburg-Landau equation.

In this illustrative problem, the sign of the nonlinear term ensures that spatially homogeneous patterns emerge from equilibrium beyond a supercritical bifurcation. In other systems, the bifurcation of such patterns may be subcritical, as it is, for example, in binary fluid convection (Thual and Fauve 1988). In these cases the equation requires further regularization if the amplitude is not to grow without bound.

2.2 Real Ginzburg-Landau equations

The complex Ginzburg-Landau equation simplifies substantially if all of the coefficients are real (so $\mu = 0$). After suitably rescaling, we then have

$$\partial_T a = \partial_X{}^2 a + (\alpha_2 - a^2)a \ , \tag{2.8}$$

where a is the real part of A. This real Ginzburg-Landau equation has been extensively studied in problems of phase separation in condensed matter physics. It has the spatially homogeneous solutions, $a = 0$ and $a = \pm\sqrt{\alpha_2}$. For $\alpha_2 > 0$, the equilibrium $a = 0$ is unstable, but the finite amplitude states are stable.

The real Ginzburg-Landau equation is of interest because it possesses solutions which take the form of fronts or kinks connecting the various homogeneous phases. The zero-amplitude equilibrium, for example, rapidly evaporates through the propagation of fronts into it which transform it to one of the stable phases (*e.g.* Ben-Jacob *et al.* 1985; van Saarloos 1989). An example of one of these fronts is shown in Fig. 1(a). Of more interest are the stationary

kink solutions, $a = K(X)$, that connect the two stable phases:

$$K(X) = \sqrt{\alpha_2}\ \tanh(X\sqrt{\alpha_2/2}) \tag{2.9}$$

(see Fig. 1(b)). The reversed solutions, $-K(X)$, are "anti-kinks." These kinks and anti-kinks persist for much longer periods of time than the "evaporation fronts" which disappear after the rapid disintegration of the unstable phase. In Benney's Eq. (2.1), they describe phase defects in the wave patterns (see Fig. 1(b)), and are the central objects of the theory of defect dynamics (*e.g.* Coullet and Elphick 1989).

The real Ginzburg-Landau equation emerged from theory of superconductivity and phase transitions. It has the form of a nonlinear diffusion equation,

$$\partial_T a - \partial_X{}^2 a = -\frac{d}{da} V(a)\ , \qquad V(a) = \frac{1}{4}a^2(a^2 - 2\alpha_2)\ . \tag{2.10}$$

On multiplying by $\partial_T a$ and integrating over X, we observe,

$$-\int (\partial_T a)^2 dX = \frac{d}{dT}\mathcal{F}\ , \tag{2.11}$$

with

$$\mathcal{F} = \int \left[(\partial_X a)^2 + V(a)\right] dX\ . \tag{2.12}$$

Since $\mathcal{F}$ is also bounded from below, it can be identified as a Lyapunov Functional for the problem, and is commonly interpreted physically as a free energy.

Depending upon boundary conditions, the existence of $\mathcal{F}$ implies that the asymptotic state of the system is typically one of the homogeneous, stable phases. This suggests that the equation is not interesting from the point of view of spatio-temporal complexity, which is not actually true. What often happens is that the evolution proceeds rapidly from some initial state as the unstable phase evaporates. This drives the system locally towards one of the two stable phases and leaves a meta-stable state consisting of multiple, phase-separated layers partitioned by a sequence of alternating kinks and antikinks. This eventually relaxes

to the asymptotic state, but in the interim, a complicated, slowly evolving pattern attains through a form of kink or frontal dynamics. Moreover, slight perturbations can sustain kink-antikink patterns indefinitely. We return to this in Sec. 4.

2.3 The cubic Schrödinger equation

In the limit of large dispersion, the Ginzburg-Landau Eq. (2.7) reduces to another well-known equation. In this limit, the large-amplitude solutions satisfy the cubic Schrödinger equation,

$$i\partial_T A = \partial_X{}^2 A + 2|A|^2 A \tag{2.13}$$

(again after rescaling). This equation has the soliton solution,

$$A = ike^{-i(\Phi-\Phi_0)} \operatorname{sech} k(X - VT + X_0) \ , \tag{2.14}$$

where the phase,

$$\Phi = \frac{1}{2} VX + \left(\frac{1}{4} V^2 - k^2\right) T \ , \tag{2.15}$$

which indicates that (2.14) is actually a two-parameter family of solitons with scale k and speed V, centered at X_0 with characteristic phase Φ_0 (*e.g.* Kivshar and Malomed 1989). One such soliton is shown in Fig. 2; it describes a localized packet or pulse of travelling waves.

The cubic Schrödinger equation is an integrable system and its soliton solutions can be studied using inverse scattering techniques (Ablowitz and Segur 1981). This allows us to generate multiple solitary-wave equilibria and consider soliton dynamics within the framework of an exact theory. In the following sections we detail an approximate method dealing with just these issues for general, dissipative PDEs. More along those lines, one can use inverse scattering theory to deal perturbatively with weakly non-integrable generalizations of (2.13). In particular, the physics of instability and dissipation appear as small forcing terms in (2.13) in the limit of large, but not infinite μ. Under such perturbations, inverse scattering theory leads to ODEs governing the evolution of the soliton's intrinsic parameters,

i.e. its position X_0, phase Φ_0, scale k and speed V (Karpman and Maslov 1977; Kaup 1976; Kivshar and Malomed 1989).

2.4 Spatio-temporal chaos in complex Ginzburg-Landau

For less specific choices of the coefficients, the complex Ginzburg-Landau equation displays a wide variety of behaviors involving coherent structures. In particular, it has become fairly important as an equation modelling spatio-temporal chaos (*e.g.* Moon *et al.* 1983; Sirovich 1989). The phenomenon is characterized by at least two regimes (Shraiman *et al.* 1992; Chaté 1994). Near the real Ginzburg-Landau limit, "phase turbulence" obtains. This appears to be a state of weak disorder reflected in the phase of A. It is closely connected to spatio-temporal chaos in the Kuramoto-Sivashinsky equation (Kuramoto 1984), which was derived as a phase-evolution equation for complex Ginzburg-Landau under certain conditions. The Kuramoto-Sivashinsky equation is the dispersionless special case of Benney's Eq. (2.1) and we consider it again in Sec. 4. In fact, in a more appropriate, moving reference frame, the phase evolution equation for complex Ginzburg-Landau turns out to be precisely Benney's equation but with an additional higher-order nonlinear term (Janiaud *et al.* 1992). Phase turbulence seems to be associated with propagating shocks or fronts in A, pulses in the gradient of its phase.

Near the highly dispersive limit, the characteristics of spatio-temporal chaos have been labelled "dispersive chaos" (Kolodner *et al.* 1990; Shöpf and Kramer 1991) or "defect turbulence" (Shraiman *et al.* 1992). The main features associated with such a state appear to be pulses which are briefly coherent in space and time. They arise through intense "self-focusing" by dispersion and subsequent breaking by dissipation (Bretherton and Spiegel 1983). In the nonlinear Schrödinger limit, these pulses probably become the solitons (2.14). Under suitable forcing, the weakly nonintegrable dynamics of these solitons do indeed show chaotic characteristics resembling the dispersive chaos of the complex Ginzburg-Landau

equation (Nozaki and Bekki 1986).

Pulses, fronts and related complex solutions are also commonly encountered in studying generalizations of the complex Ginzburg-Landau appropriate to subcritical Hopf bifurcations. A more complete survey of pulses and fronts in this kind of equation is given by van Saarloos and Hohenberg (1993). They derive families of frontal and pulse solutions in parameter space and present numerical solutions for the dynamical evolution of such objects.

3 Pulse-Train Equilibria

3.1 Pulse trains and timing maps

The arguments of the previous section concerning the common kinds of solutions to the complex Ginzburg-Landau equation suggest that Hopf bifurcations (whether subcritical or supercritical) often lead to the formation of propagating, coherent structures in spatially extended systems. Furthermore, complexity of a variety of kinds is associated with them. We now journey into theory of the patterns created by sequences of a whole ensemble of such objects, and we focus our attention upon pulses rather than kinks (minor modifications are required to treat the latter). We outline a singular perturbation theory to derive multiple solitary-wave trains, or bound states of pulses (an alternative procedure is the variational technique discussed by Kath *et al.* 1989; see also Ward 1992). We leave the question of stability until Secs. 4 and 5.

Rather than develop theory around the complex Ginzburg-Landau equation, we go back to the original model Eq. (2.1), for instabilities of a falling film. This directly illustrates how the techniques can, in principle, be used to study general partial differential systems in a single spatial dimension, not just the complex Ginzburg-Landau equation, which is strictly valid only in some region near criticality. For (2.1) with $\alpha = 0$, the spatially extended state bifurcates to instability with zero frequency. Overstability can set in, however, for spatially periodic systems as the domain size increases through a critical value (Elphick

et al. 1991a). Unstable modes saturate supercritically as nonlinear waves; they develop into solitary structures on increasing the domain size further, and this is the regime in which we operate.

When we introduce a travelling-wave coordinate $\xi = x - ct$ into (2.1) and integrate once, we find the ODE,

$$\left(\frac{d^3}{d\xi^3} + \mu\frac{d^2}{d\xi^2} + \frac{d}{d\xi}\right)\Xi - c\Xi + \frac{1}{2}\Xi^2 = 0 \ , \tag{3.1}$$

for the steady pulse train solutions, where $\Xi(\xi) = u(x,t)$.

The singular perturbation expansion centres around the idea that trains consist of widely separated pulses. The component pulses are weakly distorted versions of the true solitary waves. Single-pulse solutions centered at various positions within the train can therefore be used as a leading-order approximation to the pattern's structure (*cf.* McLaughlin and Scott 1978; Gorshkov and Ostrovsky 1982; Kawasaki and Ohta 1982; Gold'shtik and Shtern 1981; Coullet and Elphick 1989).

We let the single-pulse solution be denoted by $H(\xi)$, and choose origin so that $H(\xi)$ has its principal peak at $\xi = 0$. Away from the main peak, the pulse amplitude falls approximately exponentially. At the position of the preceding and following pulses, we assume that the amplitude is of order ε. This means that the overlap of neighboring pulses is $O(\varepsilon)$, and so the intrinsic structure of each pulse is $H(\xi) + O(\varepsilon)$. We illustrate this in Fig. 3, and write the ansatz,

$$\Xi(\xi) = \sum_k H(\xi - \xi_k) + \varepsilon R + O(\varepsilon^2) \ , \tag{3.2}$$

where ξ_k denotes the positions of the pulses and εR is the error in the basic assumption that the train is a superposition of single-pulse solutions. Were they in isolation, the pulses would move at a speed c_0. However, through interaction between the component pulses, the pattern translates differently, and $c \neq c_0$, but the disparity is small and $c = c_0 + \varepsilon c_1 + O(\varepsilon^2)$, where c_1 is order unity.

We now introduce the expansion (3.2) into the basic Eq. (3.1) and divide that equation into relations of distinct orders in ε. The leading-order equation is just that for the various single-pulse solutions. The equation at next order is a linear inhomogeneous equation for R. It has secularly divergent particular solutions unless we enforce a solvability condition upon the positions of the pulses. This condition is

$$c_1 = F(\xi_k - \xi_{k-1}) + F(\xi_k - \xi_{k+1}) \ , \tag{3.3}$$

where

$$F(\Delta) = \frac{1}{\varepsilon I} \int_{-\infty}^{\infty} N(\xi') H(\xi') H(\xi' + \Delta) d\xi' \ , \tag{3.4}$$

$N(\xi)$ is an adjoint null vector related to $H(\xi)$, and

$$I = \int_{-\infty}^{\infty} N(\xi') H(\xi') d\xi' \tag{3.5}$$

(*e.g.* Elphick, Meron and Spiegel 1990). In deriving this equation, we have tacitly assumed that the rate of decay of the pulse amplitude both fore and aft is approximately the same.

The quantites $\Delta_k \equiv \xi_k - \xi_{k-1}$ and $\Delta_{k+1} \equiv \xi_{k+1} - \xi_k$ are just an adjacent pair of pulse spacings, and so

$$F(\Delta_k) + F(-\Delta_{k+1}) = c_1 \ , \tag{3.6}$$

determines the separations of the pulses as a map of the interval of Δ to itself. This is the timing map from which we can build a pulse train. Before considering this map any further we briefly digress into the geometrical aspects of the pulse-train solution in the phase space of the dynamical system described by (3.1).

3.2 Pulse trains as dynamical systems

In order to apply the theory described above, we need to know the various kinds of single-pulse solutions, $H(\xi)$, that can arise. To find these we must study the ODE (3.1) in a little more detail.

In the phase space, $\mathbf{U} = (\Xi, \Xi', \Xi'')$, Eq. (3.1) describes a velocity field, $\mathbf{V} = \mathbf{U}'$ (where $'$ indicates differentiation with respect to argument). The divergence of the velocity field is just $-\mu$ indicating that, for $\mu > 0$, the flow is volume contracting; as time proceeds, an arbitrary set of initial points in phase space gradually condenses into a region of zero volume. The geometry restricts that region to be either a point, a curve or some surface. In other words, the system asymptotically heads towards an attractor, which could be a fixed point, a periodic orbit or a strange attractor (speaking loosely — this object is really a surface cross a Cantor set).

The attractors of the system are dependent upon the parameters of Eq. (3.1). In the context of this ODE, the parameters are μ and c (for the PDE, c is the pattern speed and only μ is a parameter). These form a two-dimensional parameter space in which the various attractors reside. They are destroyed or created at certain junctions or bifurcations, and the possibilities admitted by (3.1) are complicated (Arneodo *et al.* 1985b; Glendining and Sparrow 1984).

A sample sequence of bifurcations is shown in Fig. 4, which shows the succession of states that are realized as c is varied for $\mu = 0.7$. Initially the system contains two fixed points. That at the origin, $\Xi = 0$, is a saddle, and the nontrivial fixed point, $\Xi = 2c$, is a stable focus. Increasing c eventually destabilizes the focus, and it sheds a limit cycle (panel (a)). This cycle then bifurcates to a second cycle with twice its frequency (panel (b)) and there follows a period-doubling cascade leading to a strange attractor (panels (c) and (d)). The attractor develops as we raise c again, eventually colliding with the origin (panel (e)). Shortly after this point (panel (f)), the trajectories beginning from points in the half-space $\Xi > 0$ can find their way along a chaotic trajectory into $\Xi < 0$, and diverge to $\Xi = -\infty$ since the nonlinear term Ξ^2 cannot then saturate growth in amplitude.

In this fashion, the various attractors of the system and their bifurcations can be catalogued to visualize the kinds of propagating patterns which solve (3.1). Of primary interest

in the current context are the solutions that describe localized structures like pulses and kinks. These solutions necessarily approach constant amplitude as $\xi \to \pm\infty$, and so they must asymptote to the fixed points. The solutions that connect a fixed point to itself are the "homoclinic" orbits of the system. In real space and time, these define propagating pulses. The "heteroclinic" orbits connect different fixed points and represent kinks. Some examples are shown in Fig. 5.

The homoclinic trajectory shown in Fig. 5 connects the origin to itself. It can therefore be created by a bifurcation in which a periodic orbit collides with the origin. The details of this bifurcation are uncovered using Shil'nikov theory as we elaborate soon, but it is already clear from the sequence shown in Fig. 4 where in parameter space one might find these orbits. The strange attractor shown in Figs. 4(d) and 4(e) is densely filled with unstable periodic orbits. When it collides with the origin these periodic orbits begin connecting $\Xi = 0$ and consequently become homoclinic. For any one periodic orbit, the point of bifurcation in c typically defines a unique point at fixed μ in parameter space; this is simply the solitary-wave speed, c_0. For varying μ, we expect a curve on the parameter plane, $c_0(\mu)$.

3.3 Homoclinic dynamics

Except for a relatively short interval of time, the homoclinic solution shown in Fig. 5, $H(\xi)$, is contained within the neighborhood of the origin. Here, Eq. (3.1) can be approximately replaced by its linearization and we find the solution

$$\Xi \simeq ae^{\sigma\xi} + be^{-\gamma\xi}\cos(\omega\xi + \psi)\ , \tag{3.7}$$

where σ and $-\gamma \pm i\omega$ are the eigenvalues of the flow, and a, b and ψ are constants. The homoclinic connection emerges from the origin O at $\xi = -\infty$, escapes the vicinity of the origin, but rapidly returns and spirals back into O at $\xi = \infty$. Thus

$$H(\xi) = \begin{cases} a_0 e^{\sigma\xi} & \xi \to -\infty \\ b_0 e^{-\gamma\xi}\cos(\omega\xi + \psi_0) & \xi \to \infty \end{cases}\ . \tag{3.8}$$

The two sections of the solution for H correspond to two invariant manifolds intersecting O; a one-dimensional unstable manifold and a stable two-dimensional manifold. The homoclinic orbit is the connection of these two manifolds.

Nearly homoclinic trajectories typically get caught near the invariant manifolds, and consequently they "skirt" $H(\xi)$ during any excursion away from O. But since they generally do not re-enter the vicinity of the origin with $a = 0$ identically, the trajectories do not fall into $\Xi = 0$. Instead they become thrown out from the origin's vicinity along the unstable manifold after spending a lengthy period there. However, the reinjection process is relatively rapid, and so the solution $\Xi(\xi)$ takes on the appearance of a train of widely separated pulses. This kind of behavior is illustrated in Fig. 6. Two trajectories begin on the unstable manifold. One defines the homoclinic connection. In the second that connection is broken with $c = c_0 + \varepsilon c_1$, and the trajectory proceeds into further pulses after the first.

The nearly-homoclinic solutions spend long durations circulating near the origin, and the main peak of the pulse shadows the homoclinic's loop. This suggests that the solution can be approximately described by analytical means in the two representative regions. Near the origin we have solution (3.7), and away from it, $\Xi(\xi) \simeq H(\xi)$. In this approximation the outer part of the path is insensitive to the details of the solution, and so the flow near $\xi = 0$ controls the dynamics. This idea is entirely equivalent to supposing the pulse train is approximately composed of single-pulse solutions, and the spacings of the pulse train are determined by the nonlocal interactions between pulses occurring in their exponentially small tails. Not surprisingly, the geometrically motivated analysis, what we call Shil'nikov theory (Shil'nikov 1965, 1970; Tresser 1984a), provides a parallel description of the pulse train.

3.4 Shil'nikov theory

The flow portrayed in Fig. 6 surrounds the unstable manifold emerging from the origin. In the homoclinic condition, this manifold connects to the stable manifold. In the nearly

homoclinic conditions in which we operate, the two manifolds do not meet, but twist around one another in a complicated geometrical way. The details of this complex topology are very difficult to unravel and the dynamics of the flow is usually extracted by other means. In Shil'nikov theory, we place a surface through the phase space and determine the succession of intersections of a trajectory with it. This surface is an example of a Poincaré section. Moreover, the relation between the coordinates of successive intersections is a return map which completely characterizes the flow.

Within the cylindrical region $\mathcal{C}$, the flow is dictated by the linear system,

$$\dot{x}_1 = -\sigma x_1 + \omega x_2 \ , \tag{3.9}$$

$$\dot{x}_2 = -\sigma x_2 - \omega x_1 \tag{3.10}$$

and

$$\dot{x}_3 = \gamma x_3 \ , \tag{3.11}$$

with σ, ω and γ real and positive. There is a linear transformation between the two sets of coordinates, $\mathbf{U}$ and (x_1, x_2, x_3). In this way, the coordinate axes of $\mathbf{x}$ are the invariant manifolds of the flow within $\mathcal{C}$. In particular the homoclinic orbit departs $\mathcal{C}$ along the x_3-axis, then returns and spirals back into O in the $x_1 - x_2$ plane. Likewise, the flow leaves $\mathcal{C}$ through its top surface, shadows the homoclinic orbit, and then re-enters the vicinity of the origin through the lateral surface of $\mathcal{C}$.

The central domain $\mathcal{C}$ is bounded by the surfaces, $x_1^2 + x_2^2 = \varepsilon^2 r^2$ and $x_3 = \varepsilon Z_0$. Within it, the flow geometry is given by,

$$x_1 = \varepsilon r e^{-\sigma(\xi - \tilde{\xi}_k)} \sin[\omega(\xi - \tilde{\xi}_k) + \varphi_k] \ , \tag{3.12a}$$

$$x_2 = \varepsilon r e^{-\sigma(\xi - \tilde{\xi}_k)} \cos[\omega(\xi - \tilde{\xi}_k) + \varphi_k] \tag{3.12b}$$

and

$$x_3 = \varepsilon Z_k e^{\gamma(\xi - \tilde{\xi}_k)} \ , \tag{3.12c}$$

for some constants $\tilde{\xi}_k$ and Z_k. $\tilde{\xi}_k$ records the "time" of re-injection into $\mathcal{C}$, the instant when the trajectory intersects the curved surface. This surface acts as our Poincaré section, and the remaining two "constants", Z_k and φ_k, are the section's (cylindrical) coordinates which become known iteratively through a map of the plane.

Trajectories exit $\mathcal{C}$ at the top surface and the interval in ξ spent within $\mathcal{C}$ is given by

$$T_k = -\frac{1}{\gamma}\log(Z_k/Z_0)\ . \tag{3.13}$$

It now remains to connect the values of φ_k and Z_k with their subsequent values. In Shil'nikov theory, one normally makes some simplifying assumptions regarding the flow outside $\mathcal{C}$. This amounts to linearly relating the coordinates on the upper surface of $\mathcal{C}$ to φ_{k+1} and Z_{k+1} (*e.g.* Arneodo *et al.* 1985b), and leads to,

$$\varphi_{k+1} = \varphi_0 + qe^{-\sigma T_k}\sin(\omega T_k + \varphi_k + \Psi_1) \tag{3.14}$$

and

$$Z_{k+1} = \varepsilon C + Qe^{-\sigma T_k}\sin(\omega T_k + \varphi_k + \Psi_2)\ , \tag{3.15}$$

where q, Q, Ψ_1 and Ψ_2 are four new constants. These two equations constitute a map of the Poincaré section into itself; the advertized return map. Because of the simplifications, the constants must be treated as parameters.

3.5 Return maps versus timing maps

Although we suggested earlier that the two ways to analyse pulse train equilibria ran parallel, the timing map (3.6) is quite clearly not equivalent to the two-dimensional return map (3.14)–(3.15). The reason for this is that the Shil'nikov theory is not strictly consistent in retaining terms of similar asymptotic order. In order for the pulses to be widely separated, the interval in ξ spent within $\mathcal{C}$ must be longer than the traversal time outside it. This means that T_k is relatively long, and so the exponentials, $\exp(-\sigma T_k)$ are small, in fact of order ε. Glancing

back at Eq. (3.14) for the phase coordinate φ_{k+1} reveals that, to this order, $\varphi_k \sim \varphi_0$, and so,

$$Z_{k+1} = \varepsilon C + Qe^{-\sigma T_k} \sin(\omega T_k + \varphi) \ , \tag{3.16}$$

where $\varphi = \varphi_0 + \Psi_2$ and T_k is given by (3.13). Thus the Shil'nikov return map reduces to a map of the interval. This reflects what amounts to a local, strong "contraction" of nearby points in phase space towards the curve $\varphi_k = \varphi_0$ on the Poincaré section.

The interval spent outside C is essentially a constant, ξ_R, and so the "flight time" between the successive intersections with the Poincaré section is $\Delta_k = T_k + \xi_R$. With this quantity as map variable, we find,

$$d_1 e^{-\gamma \Delta_{k+1}} + d_2 e^{-\sigma \Delta_k} \cos(\omega \Delta_k + \phi) = \varepsilon C \ , \tag{3.17}$$

for constants d_1, d_2 and ϕ. If we introduce the asymptotic forms given by Eq. (3.8) into $F(\Delta)$, just this equation follows, with $c_1 = \varepsilon C$.

In the limit of widely separated pulses, the two approaches therefore lead to similar results. The singular perturbation theory is more powerful than conventional Shil'nikov theory in that one can compute the function $F(\Delta)$ without any free parameters (though in principal we could extend Shil'nikov's theory). Shil'nikov analysis reveals that the underlying map describing the flow is truly two-dimensional, and it is only through strong contraction that it appears one-dimensional. As a consequence, the timing maps which one extracts from numerical solution of an ODE like (3.1) appear one-dimensional only to leading order in ε. Magnifying a piece of such an "empirical map" reveals hidden fractal structure which is the signature of higher dimension (Balmforth *et al.* 1994).

3.6 Bifurcation theory

The one-dimensional return map (3.16) is often called Shil'nikov's map. We write it more explicitly as

$$Z_{k+1} = C + BZ_k^{\delta} \sin(\Omega \log Z_k + \Phi) \equiv f(Z_k) \ , \tag{3.18}$$

where B and Φ are constants, and $\delta = \gamma/\sigma$ and $\Omega = \omega/\delta$. The map is illustrated in Fig. 7 for $C = 0$ in the two cases $\delta > 1$ and $\delta < 1$.

Using the map (3.26) we can also predict the bifurcation sequence that creates the homoclinic orbit (Glendinning and Sparrow 1984). The homoclinic connection is achieved when a periodic orbit collides with the origin. Since a periodic orbit intersects the Poincaré section only a limited number of times, the orbit occurs as a recurrent iteration in the map, with the number of intersections giving the number of distinct iterations. The fixed points of the map, $Z = Z_k = Z_{k+1} = f(Z)$, correspond to the lowest-order periodic orbits of (3.1). Such an orbit hits the Poincaré section at a single point, and its period is $\Pi = \xi_R - \log(Z/Z_0)/\gamma$. If we view C as a bifurcation parameter, then (3.26) predicts the behavior of the periodic orbit as C scans through the homoclinic value (insets of Fig. 7).

When $\delta > 1$, Z monotonically approaches 0 as C decreases to homoclinicity. The orbital period Π simultaneously diverges (inset of Fig. 7a). In other words, the homoclinic connection is created by a single periodic orbit colliding with the origin and annihilating.

For $\delta < 1$, there are an infinite number of fixed points in the map at $C = 0$, and one of these periodic orbits winds into homoclinicity (inset of Fig. 7b). The winding locus of the periodic orbit represents an infinite sequence of saddle-node bifurcations and this creates the infinite number of fixed points in the map at $C = 0$. The stability of these orbits is dictated by the slope of the map. From $f'(Z)$, we observe that at each saddle-node bifurcations, every orbit is stable. Shortly beyond these points along the locus, the orbit loses stability in a period-doubling cascade.

Precisely at $C = 0$, this sequence of bifurcation leads to infinitely many unstable periodic orbits. In the vicinity of the homoclinic connection, we therefore predict the existence of a chaotic, dense set (*i.e.* the union of the unstable periodic orbits). This is the essence of Shil'nikov's theorem r $\delta < 1$ (Shil'nikov 1965, 1970; Tresser 1984a). In this region of parameter space we icipate chaos, although the long-term stability of the set is not

determined by the theorem and we cannot claim the existence of a strange attractor. If such an object nevertheless exists, we find "Shil'nikov" or "homoclinic chaos." It is observed as a train of irregularly spaced pulses; steadily propagating, spatially chaotic patterns in the PDE.

3.7 Sample timing maps

Homoclinic chaos has been observed in numerous dynamical systems. Arneodo, Coullet and Tresser (1981) found "spiral" strange attractors in piecewise linear differential systems, and later in nonlinear ODEs (Arneodo, Coullet and Tresser, 1982; Arneodo *et al.* 1985b). Here the description, "spiral," refers to the geometrical action of the mapping (3.14)-(3.15) which twists lines of constant φ_k on the Poincaré section into spirals. The attractors were further explored by Glendinning and Sparrow (1984) and Gaspard and Nicolis (1984).

Although we have approached the problem from the physical point of view of spatial complexity in solitary wave patterns, homoclinic chaos is relevant also to systems that can be described simply by ODEs. For example, in fluid physics, Arneodo *et al.* (1985a) explored the phenomenon in a simplified model of rotating, thermohaline convection (see also Arneodo and Thual, 1985). Likewise, Knobloch and Weiss (1983) found homoclinic chaos in a reduced model of magnetoconvection. Further examples, and even experimental indications, of homoclinic chaos are described in a recent conference proceedings (Physica 62D).

In the context of our current example, the ODE (3.1), it is actually fairly difficult to find strange attractors near the homoclinic bifurcation. A sample pulse train is shown in Fig. 8; the time series and timing map are shown. The asymptotic timing map agrees with the numerically determined spacings, and both terminate after a short sequence of pulses. The train terminates because the trajectory of the solution finds a way around the stable manifold at the origin and then diverges to $\Xi \to -\infty$. On the map, the final iteration reaches negative values for Z, implying that the trajectory exits the domain $\mathcal{C}$ of Fig. 6 through its

lower surface and fails to return. Such divergence leads to the gaps that are evident in the timing map of Fig. 8(b).

Although the generic behavior of the pulse train is to terminate, by judiciously using the map, one can nevertheless find strange attractors within the flow. This amounts to locating intervals in Z or Δ which remain invariant under the action of the map (*e.g.* Fig. 9). Pulse trains with these spacings continue indefinitely, but they constitute a tiny part of the phase space and their basins of attraction are small.

The divergent behavior associated with (3.1) can be avoided if we choose a different nonlinear term. In particular, if we replace Ξ^2 with a cubic nonlinearity, the equation gains the symmetry $\Xi \to -\Xi$ (and was considered by Arneodo *et al.* 1985a). Then the homoclinic orbit $H(\xi)$ has a mirror image, $-H(\xi)$, lying predominantly in the half-space $\Xi < 0$. Traversal of the stable manifold now leads to an "anti-pulse" rather than divergence, and the prospect of finding global strange attractors is more promising. A symmetrical strange attractor is shown in Fig. 10, generated from (3.1) with cubic nonlinearity. (The unmodified timing map contains no gaps, but is double-valued, although the $Z-$map is not — Glendinning 1984; Balmforth, Ierley and Spiegel 1994.) This cubic ODE describes the steady tra lling wave solutions of a *modified* Benney equation, a model which arises in other physical c exts (Tilley *et al.* 1992).

The existence of the anti-pulse in the symmetrical version of (3.1) amounts to the presence of a mechanism that reinjects trajectories back into the vicinity of the origin on either side of the stable manifold. The reinjection process need not be nearly homoclinic, nor does it guarantee the asymptotic stability of the homoclinic strange set.

3.8 Variations

In the example we have considered so far, we ha the image of Fig. 6; the homoclinic orbit ascends fr the origin along the one-dimension unstable manifold, and then returns in a

decaying spiral within the two-dimensional stable manifold. A somewhat different picture emerges when the homoclinic trajectory winds out of the origin and descends monotonically back in. The pulse is a reversed version of our original image, and we refer to it as an "inverse Shil'nikov" orbit. A chaotic solution beginning near such an object is shown in Fig. 11 (generated from a piecewise linear equation of Tresser, 1981). The trajectory occasionally approaches the homoclinic orbit in this example, but more often than not, it wanders well away from it. As a result, the solution does not resemble a train of widely separated pulses and is difficult to analyze with singular perturbation theory. Argoul *et al.* (1987) have followed through Shil'nikov theory for these reversed orbits; complications lead to a somewhat different return map. They further announce the observation of "inverse" Shil'nikov chaos in a chemical reaction.

Pulses also need not possess oscillatory tails to either the fore or aft if the system is to admit potentially chaotic solutions. In particular, monotonically decaying homoclinic orbits are frequently encountered in systems like the Lorenz equations (*e.g.* Sparrow 1982). There, the counterpart of Shil'nikov theory has been widely adapted to understand some of the bifurcations leading to the Lorenz and related attractors (although typically those attractors themselves are far from being in a homoclinic condition). Tresser (1984b) summarizes the various kinds of homoclinic situations for flows in three dimensions.

Shil'nikov theory can also be adapted to study higher-dimensional systems. In four dimensions one anticipates homoclinic orbits with two-dimensional stable and unstable manifolds. These orbits are of special interest since potentially associated with them is a strange attractor with two positive Lyapunov exponents (Glendinning and Tresser 1985), or "hyperchaos" (a term coined by Rossler 1979). Fowler and Sparrow (1991) have derived return maps expected in the case when the pulses wind both in and out of the origin, although the added complexity probably ensures that the map is reducible only to a map of the plane. If we follow singular perturbation theory, it is not immediately clear how we can account for

this, since the analysis proceeds without any explicit statement regarding dimension, and so the theory predicts the one-dimensional timing map (3.6) even for bifocal homoclinic orbits. There is currently little work on these higher dimensional pulses, at least in dissipative systems; certain Hamiltonian systems have recently been found to possess solutions composing families of infinitely many bifocal homoclinic orbits, (Champneys and Toland, 1993).

A different step up in complexity is provided by bifurcation off the homoclinic orbit itself. Under suitable conditions, the homoclinically connected origin can lose stability even in the stable manifold. If this occurs through a Hopf bifurcation, then the origin can shed a limit cycle. As $\xi \to \infty$, the homoclinic trajectory now spirals onto this limit cycle. The "Shil'nikov-Hopf" homoclinic orbit therefore connects this limit cycle to itself (*e.g.* Gaspard and Wang 1987). Hirschberg and Knobloch (1993) derive return maps for flows in the vicinity of these connections.

At this point we begin to draw parallels with theories of intermittency. The saddle point or the limit cycle lying at the heart of the homoclinic connections are simple examples of an invariant object within the phase space. The homoclinic trajectory is a pathway that leaves and returns to this object. Nearly homoclinic solutions typically spend extended periods of time near the invariant object (quiescent phases) with sporadic, rapid excursions away from it (bursts). This picture bears much in common with views about intermittency, although in typical intermittent situations the invariant object can be more complicated or even not strictly invariant. In the original example of Manneville and Pomeau (1980), the invariant object was a periodic orbit in the Lorenz system, whilst Platt *et al.* (1993) invoke the Lorenz attractor itself as chaotic invariant subspace. Along a similar vein, Wang (1993) interprets irregular bursting in a model of a neuron.

Finally, we briefly consider heteroclinic orbits. Just as we derived timing maps and reviewed Shil'nikov theory for pulses, we can follow analogous paths for fronts, kinks and shocks. Under suitable conditions we then predict "heteroclinic chaos," again with reserva-

tions concerning asymptotic stability. Along these lines, Howard and Krishnamurti (1986) found strange attractors related to heteroclinic connections (and also homoclinic orbits) within several regimes in the parameter space of a six-dimensional model of shearing convection. One such attractor and its timing map are shown in Fig. 12. In the context of the Lorenz system, Glendinning and Sparrow (1986) used Shil'nikov theory to explore heteroclinic bifurcations. For a PDE modelling a reaction-diffusion system, Koppell and Howard (1981) considered the consequences of Shil'nikov's theorem for shock-wave patterns.

4 Pulse Dynamics

4.1 Pulse interactions

In the previous section we began discussing the possible equilibria of steadily propagating pulse trains. We then digressed substantially into theory of homoclinic orbits. Now we return to more physical aspects of pulses, and consider the dynamical evolution of patterns of pulses by extending the methods of the last section.

In order to make the problem tractable from an analytical point of view, we restrict ourselves to consider only certain kinds of pulse dynamics. In what follows, we envision an ensemble of pulses which are nearly locked into a steadily propagating pattern. However, through an initial perturbation, or perhaps an intrinsic instability, we imagine that the pulses within the pattern are in a state of dynamical adjustment. This might preclude the kinds of dynamics familiar in integrable systems, like soliton collisions. Just as importantly, we also cannot cope with pulse creation and destruction (the former of which is critical to the pulses of Benney's equation, as we shortly indicate). But to take these effects into account, we need another theory, and one is not yet available. An alternative way around this is to "patch" numerical solutions into the asymptotic theory, should they prove necessary. In this way Ward (1994) treated front collisions by substituting a numerical solution whenever the fronts approached another too closely.

The assumption of weak adjustment means that the pulses of the pattern are all travelling at roughly the same speed. Consequently, they all possess approximately the same shape, and are weak distortions of a homoclinic orbit. Thus we can once more apply singular perturbation theory to determine the positions of the pulses. However, rather than a map of equilibrium pulse spacings, we now derive a set of coupled ODEs describing the evolution of the pulse's positions (McLaughlin and Scott 1978; Gorshkov and Ostrovsky 1982; Kawasaki and Ohta 1982; Coullet and Elphick 1989; Ohta and Mimura 1990; an alternative variational technique is used by Morrison *et al.* 1984).

The original ansatz that we wrote down for the pulse-train equilibria consisted of a superposition of homoclinic solutions, $H(\xi - \xi_k)$, and a residual, εR, Eq. (3.2). The wave speed in the travelling-wave coordinate, $\xi = x - ct$, emerged as the translation velocity of the pulse pattern, and this was $O(\varepsilon)$ different from the speed of an isolated pulse, c_0. Now, since the pattern itself is not steady, there is no unique pattern speed and so we set $c = c_0$. If the pulses do settle into a fixed pattern, then this must emerge as a solution to the asymptotic equations. In order to derive these equations, we introduce a slow timescale, $\tau = \varepsilon t$, upon which the pulse readjustments occur. This timescale is slow because it occurs as a result of long-range pulse interactions. We then let the pulse position depend weakly on time through τ, and write $\xi_k = \xi_k(\tau)$.

To leading order we have insisted that every pulse in the pattern travels with speed c_0, and so the solution depends upon the timescale t only in the travelling-wave combination, ξ. As a result, when we introduce the asymptotic expansion into the governing PDE, we can integrate the PDE once again and apply a solvability condition on the $O(\varepsilon)$ terms. The only difference with the steady state theory is the replacement of the velocity correction term, $\varepsilon c_1 H_k$, with $\dot{\xi}_k H_k$, and so that condition can be written as,

$$\dot{\xi}_k = F(\Delta_k) + F(-\Delta_{k+1}) \ , \tag{4.1}$$

which is the equation of motion of the k^{th} pulse.

4.2 Sample pattern dynamics

Some examples of pulse evolution are shown in Figs. 13 and 14. The first figure shows an example of twelve pulses adjusting from a set of arbitrary initial positions. The initial separations cover a moderate range and the pulses slowly lock into a steady pattern after a phase of adjustment. In the second figure, the pulses begin with a somewhat larger spread in initial spacings. This time, the pulses first lock into three distinct, quasi-steady subgroups. The subgroups then interact much more weakly; eventually they approach one another and merge into a single steady formation.

The evolution illustrated by the second example proceeds with two disjoint time and length scales (*c.f.* Shöpf and Kramer 1991). This arises from the exponential form of the interaction, and suggests that patterns of very many pulses can evolve on a whole spectrum of scales, and creates spatio-temporal complexity (Elphick *et al.* 1989).

A typical feature of evolution under the system (4.1) is gradual locking into a steady pattern. This is only possible if such patterns exist as equilibria, and therefore if $F(\Delta_k) + F(-\Delta_{k+1}) = constant$ has nontrivial solutions. In our current example this is guaranteed by the oscillatory tail of the homoclinic pulse, and the patterns shown are just two of a multitude of existing equilibria.

The examples shown in Figs. 13 and 14 follow the adjustments of an isolated group of twelve pulses. The steady patterns to which the pulses evolve are constrained by the termination of the pattern to the left and right. This ensures that the spacings of the equilibrium pattern are mostly uniform. Different patterns result if the pulses do not compose an isolated group, for example, if the pulses are arrayed periodically (Elphick *et al.* 1989). A related problem is when pulses are sequentially generated at a fixed location. This case was studied by Elphick *et al.* (1991b) in a pacemaker model of pulse propagation in a nerve-

fibre equation, and by Chang *et al.* (1993a) who compared the predictions of (4.1) with measurements of a pattern of solitary waves on a falling fluid film (Alekseenko *et al.* 1985).

4.3 An example of frontal dynamics

An alternative kind of example is shown in Fig. 15. This follows the evolution of an ensemble of kinks and antikinks for a real Ginzburg-Landau equation (Sec. 2.2; Elphick *et al.* 1991c). The heteroclinic orbits corresponding to those kinks and antikinks monotonically decay into the fixed points. Consequently. the interaction potentials represented by $F(\Delta)$ contain no minima and so the forces between kinks and antikinks are always attractive. As a result, the kinks and antikinks drift slowly towards one another under mutual interaction. This creates slowly evolving meta-stable states. Inevitably, each state terminates in the catastrophic collision of a kink-antikink pair. This marks a violent event which cannot be captured by the asymptotic method. In Fig. 15, the collisions have been crudely treated by assuming a smooth collision of the front positions.

The collision destroys one of the layers and a new meta-stable state then begins. The succession continues until as many annihilations as possible have occurred, all internal layers have vanished and the asymptotic state attains. More mathematical aspects of the problem are discussed by Fusco and Hale (1989) and Carr and Pego (1989). Some of its statistics were studied by Nagai and Kawahara (1983).

The long-lived process illustrated in Fig. 15 was derived for pattern evolution in a thermally relaxing medium (Elphick, Regev and Spiegel 1991c). Relaxation proceeds through fairly simple, frontal dynamics which engenders the rundown of complexity. The introduction of forcing can halt such a rundown. For example, Thual and Fauve (1988) and Malomed and Neponyaschy (1990) create kink-antikink bound states by introducing small dispersive terms into the equation. Elphick, Regev and Spiegel (1991c) generate complicated steady patterns through spatially periodic forcing. In either case, we add driving terms to the equations of

motion (4.1) which change its steady solutions (the equilibrium patterns).

4.4 Spacing limitation and some setbacks

We have used the PDE (2.1) as an example throughout this review to illustrate the theory of equilibrium states and dynamics of propagating pulses. This PDE is a particularly good example because the dynamics embodied in (4.1) fails completely to describe the solution if the pulse spacings become too large. This regime is precisely where one would expect the asymptotic theory to be most accurate, and the failure illustrates some of the pitfalls one could fall into by blindly applying the asymptotic machinery. A second common pitfall concerns additional invariances in the governing equation. These lead to extra free parameters in the theory that, in principle, one should fix by singular perturbation theory along with the pulse positions which represent translational invariance. For example, (2.1) also possesses Galilean invariance, although this does not appear to modify the dynamics unless the pattern is spatially extended. In contrast, the scale invariances of the nonlinear Schrödinger equation must be taken into account in any singular perturbation theory (Keener and McLaughlin 1978; Bretherton and Spiegel 1983). Otherwise the dynamics of the solitons are of an artificially low order.

To return to our example, the dynamical theory fails because a train of widely separated pulses contains extensive regions in which the amplitude of u is essentially vanishingly small. Linear theory, however, tells us that this *vacuum state* is unstable to waves. In other words, if the pulse separations are too large, the remnant instability of the vacuum state comes into play (Toh and Kawahara 1985; Chang *et al.* 1993b). The instability generates waves that are not accounted for by weak pulse interactions, and so (4.1) fails entirely to describe the dominant dynamics.

In such situations, waves bifurcate to instability and the state resembles a mixture of pulses and "radiation modes." For large dispersion, this Hopf bifurcation is subcritical and

rapidly amplifying packets of radiation destroy the pulse conFiguration. The outcome is the violent creation of new pulses (Toh and Kawahara 1985; Toh 1987; Elphick *et al.* 1991a). The new state consists of a denser train of pulses, and radiation then damps out. This leaves an equilibrium state that can be described by the asymptotic theory.

Separation-limiting instabilities therefore seem critical only at large spacings. This calls into question solutions like that shown in Fig. 14, which are unstable, and so pulse dynamics cannot generate spatio-temporal complexity of this kind on the liquid film. But for alternative PDEs, like those describing excitable medium (*e.g.* Ohta and Mimura 1990; Meron 1993) for which the vacuum state is stable, there are no limits on separation and spatio-temporal complexity can be attained.

4.5 Radiation and chaos in the KS limit

For smaller dispersions, the bifurcation of separation-limiting radiation can be supercritical. Then we can find equilibrated states consisting of co-existing pulses and finite-amplitude wave packets. One such state is shown in Fig. 16. The radiation saturates at low amplitude, but it is sufficient to affect the tail of the pulse. This "shakes" the pulse just as the tails of neighboring pulses affect its position in a pattern. Forced oscillations of coherent structures have also been observed for fronts in reaction-diffusion systems (Nishiura and Fuji 1987; Nishiura and Mimura 1989; Elezgaray and Arneodo 1991; Ikeda and Mimura 1993; Hapsburg and Meron 1994). In that case the underlying mode which bifurcates supercritically to finite amplitude has a different physical origin than the radiation mode.

A feature of the PDE (2.1) is that the separation-limiting Hopf bifurcations occur at smaller spacings at smaller dispersion. By the time dispersion disappears (the Kuramoto-Sivashinsky or KS limit), even moderately spaced pulses are unstable. Unfortunately, in this physical regime, the characteristic rates of amplitude decay away from the centre of a pulses, σ and γ, become increasingly disparate. At $\mu = 0$, their ratio is $1/2$, and pulses

are too asymmetrical to be described by unmodified perturbation theory (Balmforth *et al.* 1994). The limit is consequently far from accessibility by the present prescription of pulse dynamics.

The inability of our theory to describe pulse dynamics in the KS limit is particularly unsatisfying because here one typically finds spatio-temporal chaos (*e.g.* Hyman *et al.* 1986; Pumir 1985); incoherent interactions between pulses and a bath of radiation may be responsible for producing such a state (Toh 1987; Elphick *et al.* 1991a). A chaotic state consisting of two pulses and three unstable (and numerous stable) radiation modes is shown in Fig. 17.

In the circumstance in which spatio-temporal chaos arises from the incoherent interaction between a set of pulses and low-level radiation, one can study the power spectrum of the state at least partly analytically. By posing an ansatz like (3.2) and assuming some statistical distribution for pulse separations, one can compute spectral characteristics that reproduce features of spectra extracted from numerical experiments. In this fashion, spectral characteristics of the KS equation were studied by Toh (1987), and similar work has been done on the complex Ginzburg-Landau equation (Kishiba *et al.* 1991) and plasma turbulence models (Shen and Nicholson 1987; Qian *et al.* 1989). This type of analysis need not be used for PDEs alone; the power spectra of homoclinic strange attractors can also be derived (Gold'shtik and Shtern 1981; Brunsden and Holmes 1987; Brunsden *et al.* 1989).

The bifurcation structure of the Kuramoto-Sivashinsky equation and its chaotic states are varied and complicated (Hyman *et al.* 1986). Our view of KS chaos as interacting pulses and radiation is excessively simplistic. For example, it is not always possible to unambiguously distinguish moving pulses from the radiation. We also cannot ignore the fact that pulses are occasionally destroyed and nucleated as a result of hard collision and violent instability (Sekimoto *et al.* 1987; Toh, 1987). Moreover, in addition to pulses like that shown in Fig. 5, there are other, multiply peaked pulses and shock solutions (Balmforth *et al.* 1994; Chang *et al.* 1993b; Hooper and Grimshaw, 1988; Kent and Elgin, 1992; Michelson, 1986) which

may also play a role in the full dynamics.

In order to understand the form of spatio-temporal chaos in the Kuramoto-Sivashinsky equation (and also in the complex Ginzburg-Landau equation in the phase-turbulent regime) it would clearly be desirable to have a useful theory of radiative pulse and frontal dynamics in the dispersionless limit. By contrast, in soliton dynamics, perturbation theory surrounding the inverse scattering transform is much more successful in accounting for the interaction between radiation and solitons (Kivshar and Malomed 1991).

In seemingly less chaotic regimes, Glazier and Kolodner (1993) have experimentally studied the interactions between wave packets and pulses in binary fluid convection. In field theory, radiation or phonons often play significant roles in kink dynamics (*e.g.* Campbell *et al.* 1986; Fei *et al.* 1993). Lately, "radiative solitons" have been found in generalizations of the Kortweg de Vries and nonlinear Schrödinger equations (Pomeau *et al.* 1988; Karpman 1993a, b). These are localized structures that are structurally intertwined with far-field radiation, and perhaps are related to Shil'nikov-Hopf orbits.

5 Some Loose Ends and Outlook

In this final section we mention some related issues to the main discussion. Our survey is not meant to be a complete one, and we only summarise some topics of particular interest. After that, we remark on the relevance of the theory to the real world.

5.1 Issues of stability

In discussing either pulses and their interactions or dynamics near homoclinic orbits within the framework of asymptotic theory, we have implicitly made an assumption regarding the stability of these special types of solutions. One circumstance in which this assumption breaks down is radiative instability, but there are other cases.

In the context of ODEs, for nearly homoclinic dynamics, there is an intrinsic notion

that trajectories in phase space hug the homoclinic orbit as they traverse the main peaks of the pulses. Then, in the geometrical vision of Shil'nikov theory, the trajectory does not deviate too wildly from $H(\xi)$ as it circulates outside of the region $\mathcal{C}$ shown in Fig. 6. In singular perturbation theory, there is no such assumption, but there is also no guarantee that the approximate solutions characterized by the timing map possess any degree of stability whatsoever. In other words, for either visualization, in order for the homoclinic solutions to be interesting, they must possess a degree of both stability and instability. Without the former, no trajectory ever remains nearly homoclinic, but without the latter, the solutions are not chaotic.

For three-dimensional homoclinics, the necessary stability is assured when the orbit possesses a large and negative Floquet exponent. When the flow in phase space contracts volumes sufficiently strongly (*i.e.* when μ is sufficiently large), one exponent is likely to be of this form. For chaos, the other nontrivial Floquet exponent should be small but positive, and Shil'nikov theory tells us that this transpires for $\delta \gtrsim 1$.

Stability of a pulse in the PDE is not the same as the stability of $H(\xi)$ in the phase space of the associated dynamical system. For pulse solutions of a PDE, the question of stability constitutes a slightly more delicate issue. Radiative instability highlights the possibility that the pulse may be a stable homoclinic orbit in the ODE, but it does not evolve accordingly. In fact, there is no reason to suppose that, in general, the pulse train is remotely stable. In Benney's equation, the supercritical bifurcation of the periodic vacuum state is partly the reason why the pulse solutions are stable at short spacing. Were that bifurcation subcritical, the train would be substantially more unstable and immediately collapse or explode.

Pulse stability is resolvable with numerical techniques. An alternative, mathematically formal procedure was described by Evans (1972, 1973a, 1973b, 1975), and has been employed in a number of model equations (*e.g.* Evans and Feroe, 1975; Swinton and Elgin 1990). In the Fitz-Hugh/Nagumo equation (*e.g.* Meron 1993), it has been established that pulses are often

stable. Interestingly, these correspond to strongly unstable homoclinic orbits, in contrast to the solitary waves of Benney's equation. Therefore, even though the nerve equation admits spatially irregular patterns of pulses (Elphick *et al.* 1991b), one cannot find strange attractors in the associated ODE (oddly enough, aside from several critical signs, that ODE closely resembles one derived as a model of convection by Moore and Spiegel (1964), which can be chaotic).

5.2 Hamiltonian dynamics and Melnikov theory

In this review we have been concerned primarily with dissipative systems. Equally well, however, we could have specialized to Hamiltonian homoclinic dynamics. The parallel of Shil'nikov theory for Hamiltonian systems is Melnikov theory (Melnikov 1963). Like Shil'nikov theory, this is a geometrically based approach to uncovering the dynamics in the vicinity of a broken homoclinic connection. The ideas are most simply illustrated for a Hamiltonian system with a single degree of freedom under periodic perturbation (*e.g.* Drazin 1993). If the unperturbed system admits a homoclinic solution, then under perturbation, the connection of the stable and unstable manifolds is broken; Melnikov theory amounts to determining the distance between the two manifolds, as measured along an axis normal to the original homoclinic orbit.

The key ingredient in Melnikov's analysis is an integral $M(t_0)$ which measures the breakage of the manifolds (t_0 parameterizes the unperturbed homoclinic orbit). This integral is commonly called Melnikov's function. If it vanishes, then we infer that the manifolds cross. Because the perturbation is also periodic, it further implies that $M(t_0)$ is likewise periodic, and so the manifolds intersect one another an infinite number of times. The entangling of the manifolds (a "homoclinic tangle") signifies the existence of chaotic orbits, and is the analogue of Shil'nikov's theorem. If the Melnikov function does not vanish, then the manifold never intersect, and more global methods are needed to study the outcome.

Melnikov theory is rather elegantly formulated in the framework of Hamiltonian dynamics. But it need not be couched in those terms (Chow *et al.* 1980). In fact, as pointed out by Coullet and Elphick (1987), the Melnikov method for dissipative systems is essentially the same as singular perturbation theory. The Melnikov function in that context is simply the integral appearing in the solvability condition; the requirement that it vanish ensures bounded solutions in the asymptotic calculation, which is equivalent to saying that the manifolds entangle. But, just as Shil'nikov theory provides more geometrical information regarding the dynamics around the homoclinic orbits than the timing map, so too does Melnikov theory.

5.3 Painlevé analysis and pole expansion

Our approach to the problem of pulse dynamics has been founded on the idea that solitary waves correspond to homoclinic orbits of the dynamical system associated to the governing PDE. Save for some special cases, these orbits need to be determined numerically, at least for most dissipative systems. This is not, however, the only approach one can take to the problem. Exact, analytical solitary solutions can also be furnished by Painlevè analysis (Weiss *et al.* 1983). Though intimately connected with integrable systems, the Painlevè method occasionally works for dissipative systems. The heteroclinic solution of the KS equation which is pictured in Fig. 5 can be uncovered in this fashion (Conte and Musette 1989), as can several solitary-wave solutions of Benney's equation at particular values of the dispersion parameter (Kudryashov 1990). The trouble with uncovering analytical solutions in this way is that it is rarely possible, and certainly gives no indication of the wealth of solutions possible. Yet when the analysis furnishes an analytical solution, it can be very useful.

A somewhat related method for pulse dynamics is pole expansion. This was first applied to derive soliton solutions for the KdV equation and some of its relatives (Kruskal 1975; Airault *et al.* 1977; Birnir 1986). Unlike approximation by homoclinic orbits, the method

centres around the idea that, by choosing an appropriate selection of rational functions, we can obtain exact nonlinear solutions. This amounts to finding a finite set of movable singular or pole solutions that solve the PDE exactly, provided their positions satisfy certain ODEs. Once again, this method only works under special circumstances, and is at least partially connected to integrability (Birnir 1986). But unlike singular perturbation theory and Eq. (4.1), the dynamical equations that one extracts with pole expansion are exact nonlinear evolution equations for the pole positions, which may or may not resemble individual pulses. In addition to the KdV equation, it has been employed to find solutions of the dissipative Benjamin-Ono equation (Meiss 1980; Lee and Chen 1982; Qian *et al.* 1989) and a variation of the Boussinesq equation (Qian and Spiegel 1994).

5.4 Something of the real world

What we have described in this review is a theory of the dynamics of homoclinic orbits in an ODE, and of pulses in a PDE. In the real world, most systems have too many degrees of freedom to be described by simple theory of this kind. For systems describable by ODEs, this is mainly the reason why there are very few examples of experimental timing maps like those pictured here, even when the object under study bursts sporadically and would appear to be close to being homoclinic (lasers dynamics has something of the flavor of homoclinic theory — Arrechi *et al.* 1993; Papoff *et al.* 1991). One important difference is that there can be intrinsic noise in experimental systems. This restricts the accessibility of phase space near the stagnation point at the origin, with critical repercussions on the timing map; lengthy spacings are prohibited and periodic orbits can change (Hughes and Proctor 1990; Stone and Holmes 1991; Arrechi *et al.* 1993).

In asymptotic theory, noise can be added perturbatively. This influences the solvability condition in a similar fashion to the perturbations of the Ginzburg-Landau equation

mentioned in Sec. 4.3. The pattern equations become

$$F(\Delta_k) + F(-\Delta_{k+1}) = c_1 + g_k \ , \tag{5.1}$$

where g_k depends on the pulse positions for deterministic perturbations, and is a stochastic variable in the case of noise. Accordingly, deterministic perturbations intrinsically change the map; noise "jitters" the spacings of a pulse train. If perturbations are excessively large, all signature of the underlying Shil'nikov map can be lost.

For a spatio-temporal system, noise can be added in a similar way. Then the equation of motion of the pulse (4.1) becomes stochastically driven, an effect like Brownian motion. This sort of phenomenon would be relevant to pulses immersed in a heat bath, a situation that might be used to model multiple, excited radiative modes in a many-pulse system.

As regards experimental observations of pulse dynamics, the situation is again difficult to compare with theory. Solitary waves on fluid films are subject to secondary instabilities which typically wrecks the possibility of recording persistent one-dimensional interaction (Chang *et al.* 1993a). In spite of this drawback, some of the results of Liu and Gollub (1994) suggest that experimental analogues might be found for fluid films. In binary fluid convection, it is invariably only a small number of pulses that emerge in the system, and it does not seem currently possible to describe these with simple PDEs.

The theory we have described is most useful in pointing to a way of completely describing spatio-temporal complexity in a simple system. Though real systems are generally substantially more complicated, the understanding gained in such a simple situation will hopefully provide invaluable insights into more physical cases. In higher dimension, things only become worse and we open Pandora's box. Geometrically alone, pulses can take shapes of all kinds, from disks and spheroids to spirals and scrolls. Weak interaction theory could provide interaction potentials necessary for the dynamics of these coherent structures, if regardable as point particles. Then many-body dynamics could be attempted. But even in one dimension,

we have seen that this often is not enough.

Acknowledgments

I thank G.R. Ierley, P.J. Morrison, E.A. Spiegel and C. Tresser for comments, conversations and criticisms.

References

Ablowitz, M.J., Segur, H. 1981, Solitons and the Inverse Scattering Transform, Philadelphia: SIAM.

Airault, H., McKean, H.P, Moser, J.E. 1977, Rational and elliptic solutions of the Kortweg de-Vries equation and a related many-body problem, *Comm. Pure App. Math.* 30: 95-148.

Alekseenko, S.V., Nakoryakov, V.Y., Pokusaev, B.G. 1985, Wave formation on a vertically falling liquid film, *A.I.Ch.E. Journal* 31: 1446-1460.

Anderson, K.E., Behringer, R.P. 1990, Long timescales in traveling-wave convection patterns, *Phys. Lett.* A145: 323-328.

Argoul, F., Arneodo, A., Richetti, P. 1987, Experimental evidence for homoclinic chaos in the Belousov-Zhabotinskii reaction, *Phys. Lett.* 120A: 269:275.

Arneodo, A., Coullet, P.H., Spiegel, E.A. 1985a, Dynamics of triple convection, *Geophys. Astrophys. Fluid Dyn.* 31: 1-48.

Arneodo, A., Coullet, P.H., Spiegel, E.A., Tresser, C. 1985b, Asymptotic chaos, *Physica D* 14: 327-347.

Arneodo, A., Coullet, P., Tresser, C. 1981, Possible new strange attractors with spiral structure, *Comm. Math. Phys.* 79: 573-579.

Arneodo, A., Coullet, P., Tresser, C. 1982, Oscillators with chaotic behavior: an illustration of a theorem by Shil'nikov, *J. Stat. Phys.* 27: 171-182.

Arneodo, A., Thual, O. 1985, Direct numerical simulations of a triple convection problem versus normal form predictions, *Phys. Lett.* 109A; 367-373.

Arrechi, F.T., Lapucci, A., Meucci, R. 1993, Poincaré versus Boltzmann in Shil'nikov phenomena, *Physica D* 62: 186-191.

Balmforth, N.J., Ierley, G.R., Spiegel EA. 1994, Chaotic Pulse Trains, *SIAM J. Appl. Math.* to appear.

Benney, D.J. 1966, Long waves on liquid films, *J. Mathematics and Physics* 45:150-155.

Ben-Jacob, E., Brand, H., Dee, G., Kramer, L., Langer, J.S. 1985, Pattern propagation in nonlinear dissipative systems, *Physica D* 14: 348-364.

Bensimon, D., Kolodner, P., Surko, C.M., Williams, H., Croquette, V. 1990, Competing and co-existing dynamical states of travelling-wave convection in an annulus, *J. Fluid Mech.* 217: 441-467.

Birnir, B. 1986, Chaotic perturbations of KdV 1. Rational solutions, *Physica D* 19: 238-254.

Bretherton, C.S., Spiegel, E.A. 1983, Intermittency through modulational instability, *Phys. Lett.* 96A: 152-156.

Brunsden, V., Cortell, J., Holmes, P.J. 1989, Power spectra of chaotic vibrations of a buckled beam, *J. Sound Vib.* 130: 1-25.

Brunsden, V., Holmes, P. 1987, Power spectra of strange attractors near homoclinic orbits, *Phys. Rev. Lett.* 58: 1699-1702.

Campbell, D.K., Peyrard, M., Sodano, P. 1986, Kink-antikink interactions in the double sine-Gordon equation, *Physica D* 19: 165-205.

Carr, J., Pego, R.L. 1989, Meta-stable patterns in solutions of $u_t = \varepsilon^2 u_x x - f(u)$, *Comm. Pure App. Math.* 17: 523-576.

Champneys, A.R., Toland, J.F. 1993, Bifurcation of a plethora of multi-modal homoclinic orbits for autonomous Hamiltonian systems, *Nonlinearity* 6: 655-721.

Chang, H-C. 1994, Wave evolution on a falling film, *Ann. Rev. Fluid Mech.* 26: 103-136.

Chang, H-C., Demekhim, E.A., Kopelevich, D.I. 1993a, Nonlinear evolution of waves on a vertically falling film, *J. Fluid Mech.* 250: 433-480.

Chang, H-C, Demekhim, E.A., Kopelevich, D.I. 1993b, Laminarizing effects of dispersion in an active-dissipative nonlinear medium, *Physica D* 63: 299-320.

Chaté, H. 1994, Disordered regimes of the one-dimensional complex Ginzburg-Landau equation, *Nonlinearity* to appear.

Chow, S.N., Hale, J.K., Mallet-Paret, J. 1980, An example of bifurcation to homoclinic orbits, *J. Diff. Eq.* 37: 351-373.

Coullet, P., Elphick, C. 1987, Topological defect dynamics and Melnikov's theory, *Phys. Lett.* 121A: 233-236.

Coullet, P., Elphick, C. 1989, Rhythms and pattern transitions, *Physica Scripta* 40: 398-408.

Conte, R., Musette, M. 1989, Painlevé analysis and Bäcklund transformation in the Kuramoto-Sivashinsky equation, *J. Phys A* 22: 169-177.

Drazin, P.G. 1993, *Nonlinear Systems*, Cambridge: Cambridge Univ. Press.

Elezgaray, J., Arneodo, A. 1991, Modelling reaction-diffusion pattern formation in the Couette flow reactor, *J. Chem. Phys.* 95: 323-350.

Elphick, C., Ierley, G.R., Regev, O., Spiegel, E.A. 1991a, Interacting localized structures with Galilean invariance, *Phys. Rev. A* 44: 1110-1122.

Elphick, C., Meron, E., Rinzel, J., Spiegel, E.A., 1991b, Impulse patterning and relaxational propagation in excitable media, *J. Theor. Biol.* 146: 249-268.

Elphick, C., Meron, E., Spiegel, E.A. 1989, Spatio-temporal complexity in travelling patterns, *Phys Rev. Lett.* 61: 496-499.

Elphick, C., Meron, E., Spiegel, E.A. 1990, Patterns of propagating pulses, *SIAM J. Applied Math.* 50: 490-503.

Elphick, C., Regev, O., Spiegel, E.A. 1991c, Complexity from thermal instability, *Monthly Notices R.A.S.* 250: 617-628.

Evans, J.W. 1972, Nerve axon equations I: Linear approximations, *Indiana Univ. Math. J.* 21: 877-885.

Evans, J.W. 1973a, Nerve axon equations II: Stability at rest, *Indiana Univ. Math. J.* 22: 75-90.

Evans, J.W. 1973b, Nerve axon equations III: Stability of the nerve impulse, *Indiana Univ. Math. J.* 22: 577-593.

Evans, J.W. 1975, Nerve axon equations IV: The stable and the unstable impulse, *Indiana Univ. Math. J.* 24: 1169-1190.

Evans, J.W., Feroe, J.A. 1977, Local stability theory of the nerve impulse, *Math. Biosc.* 37: 23-50.

Fei, Z., Konotop, V.V., Peyrard, M., Vásquez, L. 1993, Kink dynamics in the periodically modulated ϕ^4 model, *Phys. Rev. A* 48: 548-554.

Flesselles, J-M., Simon, A.J., Libchaber, A.J. 1991, Dynamics of one-dimensional interfaces: an experimentalist's view, *Adv. Phys.* 40: 1-51.

Fowler, A.C., Sparrow, C.T. 1991, Bifocal homoclinic orbits in four dimensions, *Nonlinearity* 4: 1159-1182.

Fusco, G., Hale, J.K. 1989, Slow-motion manifolds, dormant instability, and singular perturbations, *J. Dyn. Diff. Equ.* 1: 75-94.

Gaspard, P., Nicolis, G. 1983, What can we learn from homoclinic orbits in chaotic dynamics? *J. Stat. Phys.* 31: 499-518.

Gaspard, P., Wang, X-L. 1987, Homoclinic orbits and mixed-mode oscillations in far-from-equilibrium systems, *J. Stat. Phys.* 48: 151-191.

Glazier, J.A., Kolodner, P. 1993, Interactions of nonlinear pulses in convection in binary fluids, *Phys. Rev. A* 48: 4269-4280.

Glendinning, P. 1984, Bifurcations near homoclinic orbits with symmetry, *Phys. Lett.* 103A: 163-166.

Glendinning, P., Sparrow, C.T. 1984, Local and global behavior near homoclinic orbits, *J. Stat. Phys.* 35: 645-696.

Glendinning, P., Sparrow, C.T. 1986, T-points: A co-dimension two heteroclinic bifurcation, *J. Stat. Phys.* 43: 479-488.

Glendinning, P., Tresser, C. 1985, Heteroclinic loops leading to hyperchaos, *J. Physique* 46: L347-352.

Gol'dshtik, M.A., Shtern, V.N. 1981, Theory of structural turbulence, *Sov. Phys. Dokl.* 257: 1319-1322.

Gorshkov, K.A., Ostrovsky, L.A. 1981, Interactions of solitons in non-integrable systems: direct perturbation method and applications, *Physica D* 3: 424-438.

Hapsberg, A., Meron, E. 1994, Pattern formation in dissipative nonvariational systems: the effects of front bifurcations, *Phys. Rev. E* submitted.

Hirschberg, P., Knobloch, E. 1993, Shil'nikov-Hopf bifurcation, *Physica D* 62: 202-216.

Hooper, A.P., Grimshaw, R. 1988, Travelling wave solutions of the Kuramoto-Sivashinsky equation, *Wave Motion* 10: 405-420.

Howard, L.N., Krishnamurti, R. 1986, Large-scale flow in turbulent convection: a mathematical model, *J. Fluid Mech.* 170: 385-410.

Hughes, D.W., Proctor, M.R.E. 1990, A low-order model of the shear instability of convection: chaos and the effect of noise, *Nonlinearity* 3: 127-154.

Hyman, J.H., Nicolenko, B., Zaleski, S. 1986, Order and complexity in the Kuramoto-Sivashinsky model of weakly turbulent interfaces, *Physica D* 23: 265-292.

Ikeda, T., Mimura, M. 1993, An interfacial approach to regional segregation of two competing species mediated by a predator, *J. Math. Biol.* 31: 215-240.

Janiaud, B., Pumir, A., Bensimon, D., Croquette, V., Richter, H., Kramer, L. 1992, The Eckhaus instability for travelling waves, *Physica D* 55: 269-286.

Joets, A., Ribotta, R. 1988, Localized, time-dependent state in the convection of a nematic liquid crystal, *Phys. Rev. Lett.* 60: 2164-2167.

Karpman, V.I. 1993a, Radiation by solitons due to higher-order dispersion, *Phys. Rev. E* 47: 2073-2082.

Karpman, V.I. 1993b, Stationary and radiating dark solitons of the third order Schrödinger equation, *Phys. Lett.* 181A: 211-215.

Karpman, V.I, Maslov, E.M. 1977, Perturbation theory of solitons, *Soviet Phys. JETP* 46: 281-291.

Kath, W.L, Knessl, C., Matkowsky, B.J. 1987, A variational approach to nonlinear singularly perturbed boundary-value problems, *Studies Appl. Math.* 77: 61-88.

Kaup, 1976, A perturbation expansion for the Zhakarov-Shabat inverse scattering transform, *SIAM J. Appl. Math.* 31: 121-133.

Kawahara, T., Toh, S. 1987, Pulse interactions in an unstable dissipative-dispersive nonlinear system, *Phys. Fluids* 31: 2103-2111.

Kawasaki, K., Ohta, T. 1982, Kink dynamics in one-dimensional nonlinear systems, *Physica A* 116: 573-593.

Keener, J.P., McLaughlin, D.W. 1977, Solitons under perturbations, *Phys. Rev. A* 16: 777-790.

Kent, P., Elgin, J. 1992, Travelling-wave solutions of the Kuramoto-Sivashinsky equation: period-multiplying bifurcations, *Nonlinearity* 4: 899-920.

Kishiba, S., Toh, S., Kawahara, T. 1991, An estimate of energy spectra of the Ginzburg-Landau chaos, *Physica D* 54: 43-57.

Kivshar, Y.S., Malomed, B.A. 1989, Dynamics of solitons in nearly integrable systems, *Rev. Mod. Phys.* 61:763-918.

Knobloch, E., Weiss, N. 1983, Bifurcations in a model of magnetoconvection, *Physica D* 9: 379-407.

Kolodner, P. 1991a, Drift, shape, and intrinsic destabilization of pulses of travelling-wave convection, *Phys. Rev. A* 44: 6448-6465.

Kolodner, P. 1991b, Collisions between pulses of travelling-wave convection, *Phys. Rev. A* 44: 6466-6479.

Kolodner, P., Glazier, J.A., Williams, H. 1990, Dispersive chaos in one-dimensional travelling-wave convection, *Phys. Rev. Lett.* 65: 1579-1582.

Kopell, N., Howard, L.N. 1981, Target patterns and horse shoes from a perturbed central-force problem: some temporally periodic solutions to reaction-diffusion equations, *Studies in Applied Math.* 64: 1-56.

Kruskal, M.D. 1975, In *Nonlinear wave motion*, ed. Newell AC (American Mathematical Society, Providence RI), Vol. 15: 61-83.

Kudryashov, N.A. 1990, Exact solutions of the generalized Kuramoto-Sivashinsky equation, *Phys. Lett.* 147A: 287-291.

Kuramoto, Y. 1984, *Chemical Oscillations, Waves and Turbulence*, Berlin: Springer.

Lee, Y.C., Chen H.H. 1982, Nonlinear dynamical models of plasma turbulence, *Physica Scripta* T2/1: 41-47.

Liu, J., Gollub, J.P. 1994, Solitary wave dynamics of film flows, Preprint.

Liu, J., Paul, J.D, Gollub, J.P. 1993, Measurements of the primary instabilities of film flows, *J. Fluid Mech.* 250:69-101.

Malomed, B., Nepomnyashchy, A.A. 1990, Kinks and solitons in the generalized Ginzburg-Landau equation, *Phys. Rev. A.* 42: 6009-6014.

Manneville, P. 1990, *Dissipative Structures and Weak Turbulence*, New York: Academic.

Manneville, P., Pomeau, Y. 1980, Different ways to turbulence in dissipative dynamical systems, *Physica D* 1: 219-226.

McLaughlin, D.W., Scott, A.C. 1978, Perturbation analysis of fluxon dynamics, *Phys. Rev. A* 18: 1652-1680.

Meiss, J.D. 1980, Rational solutions to some partial differential equations, In *Geophysical Fluid Dynamics*, WHOI 80-53 (Woods Hole Oceanographic Institution): 155-164.

Melnikov, V.K., 1963, On the stability of the centre for time periodic perturbations, *Trans. Moscow Math.* 12: 1-57.

Meron, E. 1993, Pattern formation in excitable media, *Phys. Reports* 218: 1-66.

Michelson, D. 1986, Steady solutions of the Kuramoto-Sivashinsky equation, *Physica D* 19: 89-111.

Moon, H.T., Huerre, P., Redekopp, L.G. 1983, Transition to chaos in the Ginzburg-Landau equation, *Physica D* 7: 135-152.

Moore, D.W., Spiegel, E.A. 1966, A thermally excited nonlinear oscillator, *Astrophys. J.* 143: 871-887.

Morrison, P.J., Meiss, J.D., Cary, J.R. 1984, Scattering of regularized-long-wave solitary waves, *Physica D* 11: 324-336.

Moses, E., Fineberg, F., Steinberg, V. 1987, Multistability and confined travelling-wave patterns in a convecting binary mixture, *Phys. Rev. A* 35: 2757-2760.

Nagai, T., Kawasaki, K. 1983, Molecular dynamics of interacting kinks I, *Physica A* 120: 387-399.

Niemela, J.J., Ahlers, G., Cannell, D.S. 1990, Localized traveling-wave states in binary-fluid convection, *Phys. Rev. Lett.* 64: 1365-1368.

Nishiura, Y., Fuji, H. 1987, Stability of singularly perturbed solutions to systems of reaction-diffusion equations, *SIAM J. Math. Anal.* 18: 1726-1770.

Nishiura, Y., Mimura, M. 1989, Layer oscillations in reaction-diffusion systems, *SIAM J. Appl. Math.* 49: 482-514.

Nozaki, K., Bekki, N. 1986, Low-dimensional chaos in a driven damped nonlinear Schrödinger equation, *Physica D* 21: 381-393.

Ohta, T., Mimura, M. 1990, Pattern dynamics in excitable media, *Formation, dynamics and statistics of patterns.* Vol. 1, 55-112. Ed. K. Kuramoto *et al.* World Scientific.

Papoff, F., Fioretti, A., Arimondo, E. 1991, Return maps for intensity and time in a homoclinic-chaos model applied to a laser with a saturatable absorber, *Phys. Rev. A* 44: 4369-4651.

Platt, N., Spiegel, E.A., Tresser, C. 1993, On-off intermittency: a mechanism for bursting, *Phys. Rev. Lett.* 70: 279-282.

Pomeau, Y., Ramani, A., Grammaticos, B. 1988, Structural stability of the Kortweg-de Vries solitons under a singular perturbation, *Physica D* 31: 127-134.

Pumir, A. 1985, Statistical properties of an equation describing fluid interfaces, *J. Physique* 46: 511-522.

Qian, S., Lee, Y.C., Chen H.H. 1989, A study of nonlinear dynamical models of plasma turbulence, *Phys. Fluids B* 1: 87-98.

Qian, Z.S., Spiegel, E.A. 1994, Autogravity waves in a polytropic slab, *Geophys. Astrophys. Fluid Dyn.* to appear.

Rossler, O.E. 1979, An equation for hyperchaos, *Phys. Lett.* 71A: 155-157.

Sekimoto, K., Kawasaki, K., Ohta, H. 1987, Aspects of nucleation and drift processes in a one-dimensional model, *J. Stat. Phys.* 48: 1213-1241.

Shen, M-M., Nicholson, D.R. 1987, Numerical comparison of strong Langmuir turbulence models, *Phys. Fluids* 30: 1096-1103.

Shil'nikov, L.P. 1965, A case of the existence of a countable number of periodic motions, *Soc. Math. Dokl.* 6: 163-166.

Shil'nikov, L.P. 1970, A contribution to the problem of the structure of an extended neighborhood of a rough equilibrium state of saddle-focus type, *Math. USSR Sbornik* 10: 91-102.

Shöpf, W., Kramer, L. 1991, Small-amplitude periodic and chaotic solutions of the complex Ginzburg-Landau equation for a subcritical bifurcation, *Phys. Rev. Lett.* 66: 2316-2319.

Shraiman, B., Pumir, A., van Saarloos, W., Hohenberg, P.C., Chaté, H., Holen, M. 1992, Spatiotemporal chaos in the one-dimensional complex Ginzburg-Landau equation, *Physica D* 57: 241-248.

Sirovich, L. 1989, Chaotic dynamics of coherent structures, *Physica D* 37: 126-145.

Sparrow, C. 1982, *The Lorenz Equations: bifurcations, chaos and strange attractors*, New York: Springer-Verlag.

Stone, E., Holmes, P. 1991, Unstable fixed points, heteroclinic cycles and exponential tails in turbulence production, *Phys. Lett.* 155A: 29-42.

Swinton, J., Elgin, J. 1990, Stability of travelling pulse solutions to a laser equation, *Phys. Lett.* 145A: 428-433.

Thual, O., Fauve, S. 1988, Localized structures generated by subcritical instabilities, *J. Physique* 49: 1829-1833.

Tilley, B.S., Davis, S.H., Bankoff, S.G. 1992, Stability of stratified fluids in an inclined channel, *Bull. Am. Phys. Soc.* 37: 1718.

Toh, S. 1987, Statistical model with localized structures describing the spatio-temporal chaos of Kuramoto-Sivashinsky equation, *J. Phys. Soc. Jpn.* 56: 949-962.

Toh, S., Kawahara T. 1985, On the stability of soliton-like pulses in a nonlinear dispersive system with instability and dissipation, *J. Phys. Soc. Jpn.* 54: 1257-1269.

Tresser, C. 1981, Ph.D. Thesis, Univ. of Nice.

Tresser, C. 1984a, About some theorems of Shil'nikov, *Ann. Inst. H. Poincaré* 40: 441-461.

Tresser, C. 1984b, Homoclinic orbits for flows in $\mathbb{R}^3$, *J. Physique* 45: 837-841.

van Saarloos, W. 1989, Front propagation into unstable states: marginal stability as a dynamical mechanism for velocity selection, *Phys. Rev. A* **37:** 211-229.

van Saarloos, W., Hohenberg P. 1993, Fronts, pulses, sources and sinks in generalized Ginzburg-Landau equations, *Physica D* 56: 303-347.

Wang, X-J. 1993, Genesis of bursting oscillations in the Hindmarsh-Rose model and homoclinicity to a chaotic saddle, *Physica D* 62: 263-274.

Ward, M.J. 1992, Eliminating indeterminacy in singularly perturbed boundary value problems with translational invariant potentials, *Stud. Appl. Math.* 87: 95-134.

Ward, M.J. 1994, Metastable patterns, layer collapses, and coarsening for a one-dimensional Ginzburg-Landau equation, *Studies Appl. Math.* 91: 51-93.

Weiss, J,, Tabor M, Carnevale G. 1983, The Painlevé property for partial differential equations, *J. Math. Phys.* 24: 522-526.

Wu, J., Keolian, R., Rudnick, I. 1984, Observation of a nonpropagating hydrodynamic soliton, *Phys. Rev. Lett.* 52: 1411-1424.

Figure Captions:

1. Kink solutions of the real Ginzburg-Landau equation. Panel (a) shows an "evaporation front" connecting the unstable and stable phases. Panel (b) shows a kink connecting the two stable phases.

2. Soliton solution of the nonlinear Schrödinger equation.

3. Pulse train and ansatz ($H_k = H(\xi - xi_k)$.)

4. Bifurcation sequence of Eq. (3.1) for $\mu = 0.7$ and six values of c. The six panels show phase portraits projected onto a plane with coordinates $(\Xi, \dot{\Xi} + \ddot{\Xi}/4)$. The stars mark the fixed points.

5. Homoclinic and heteroclinic solutions of (3.1). Panel (a) shows the homoclinic orbit and its pulse-like time trace. Panel (b) shows the heteroclinic orbit and its frontal time trace. The orbits are shown projected onto the $(\Xi, \dot{\Xi})$ plane. The stars show the fixed points.

6. Homoclinic dynamics. Panel (a) shows the homoclinic orbit $H(\xi)$ and a nearly homoclinic trajectory $\Xi(\xi)$ beginning from the unstable manifold of the origin. The cylindrical central region $\mathcal{C}$ is identified. Panel (b) shows a magnification of the region surrounding $\mathcal{C}$. Panel (c) compares the time traces of the two solutions.

7. Shil'nikov's map for (a) $\delta = 2$ and (b) $\delta = 0.5$. The inset panels indicate the behavior of a fixed point of the map as C varies, and the distance to homoclinicity changes (so illustrating the bifurcation sequence).

8. Sample pulse train plus maps. Panel (a) shows the pulse train. Panel (b) shows the associated timing map. The curves indicate the asymptotic map, the stars and iteration show the computed spacings.

9. An invariant set.

10. A cubic invariant set for Eq. (3.1), but with cubic nonlinearity. Panel (a) shows the empirical (measured) timing map. Panel (b) shows the phase portrait projected onto the $(\Xi, \dot{\Xi})$ plane. The stars indicate the fixed points. Panel (c) presents part of the pulse-antipulse train.

11. The time trace of a chaotic solution in the vicinity of an inverse Shil'nikov homoclinic orbit (adapted from Tresser 1981). Not shown is a nearly homoclinic precursor.

12. Heteroclinic chaos in the Howard-Krishnamurti model. Panel (a) shows a phase portrait projected onto the (A, B) plane. Panel (b) displays the time trace of A. Panel (c) is the empirical (measured) timing map.

13. Evolution of twelve pulse. Panel (a) shows the evolution of the positions, panel (b) the final pattern.

14. An example of the evolution of 12 pulses from arbitrary initial conditions. Initially, the pulses lock into 3 almost steady subgroups (panel (a)). Then these subgroups eventually collide into a single formation (panel (b)) with the pattern shown in (c). In panel (b), a synchronized drift in the position of all of the pulses has been subtracted out.

15. Frontal dynamics. Panel (a) shows the positions of the fronts as they initially evolve and collide. Panel (b) shows the eventual evolution and annihilation of the remaining four fronts after the intial phase. Panel (c) shows the initial kink-antikink conFiguration.

16. A pulse with a supercritically saturated radiative instability. Shown is a space-time surface plot.

17. A two pulse chaotic state. Shown is a space-time surface plot. Time recedes into the page; space increases to the right.

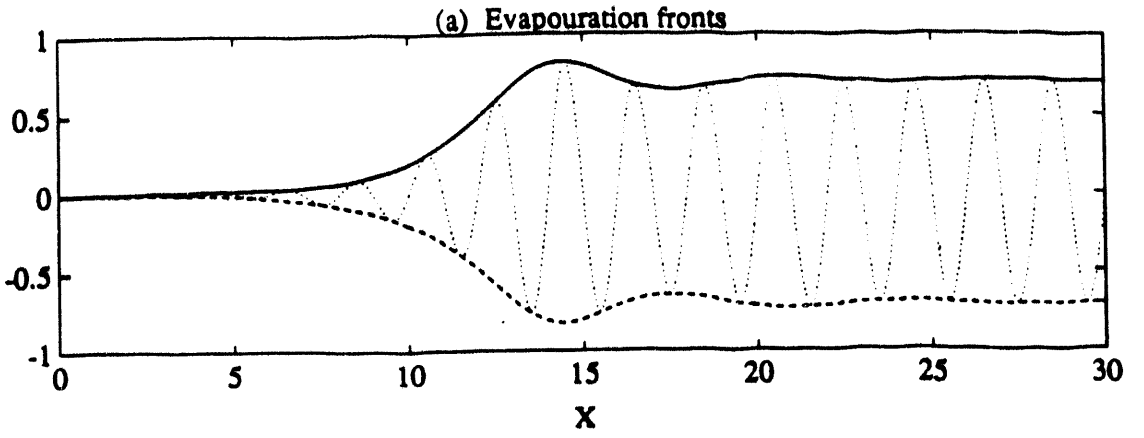
(a) Evapouration fronts
1
0.5
0
-0.5
-1
0
5
10
15
20
25
30
X

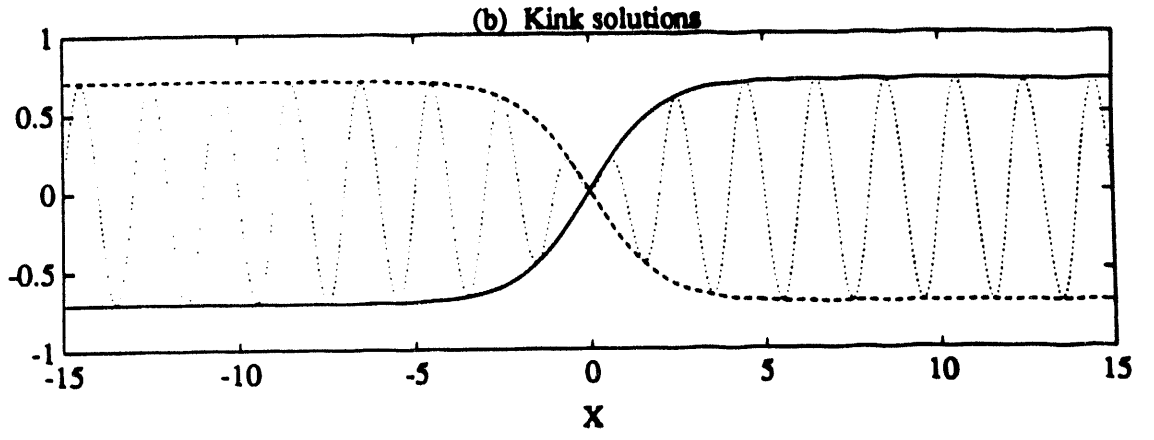
(b) Kink solutions
1
0.5
0
-0.5
-1
-15
-10
-5
0
5
10
15
X

Figure 1

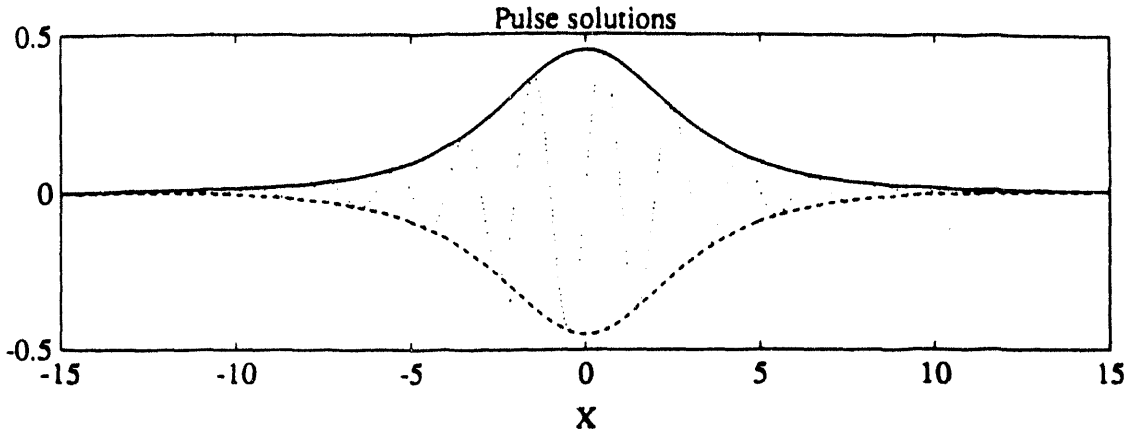

Fig. 2

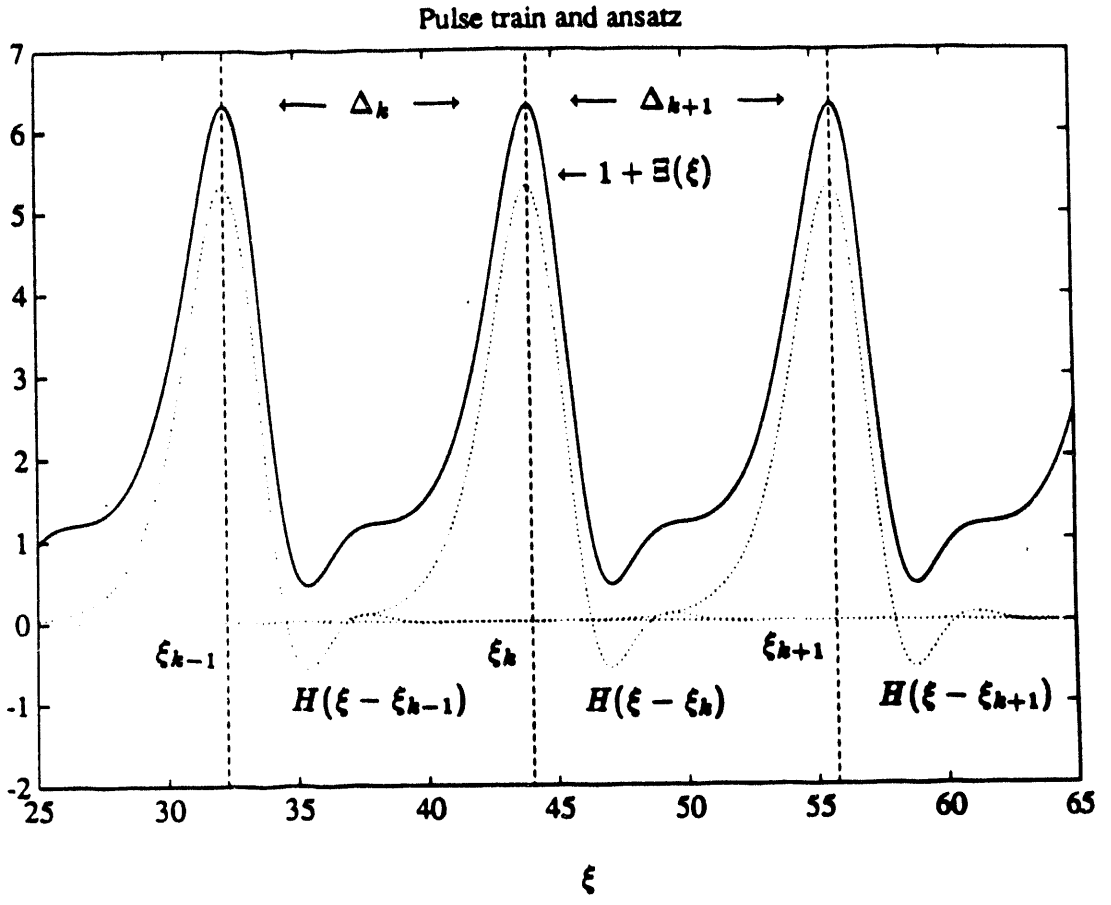
Pulse train and ansatz
Δ_k
Δ_{k+1}
$1 + \Xi(\xi)$
ξ_{k-1}
ξ_k
ξ_{k+1}
$H(\xi - \xi_{k-1})$
$H(\xi - \xi_k)$
$H(\xi - \xi_{k+1})$
7
6
5
4
3
2
1
0
-1
-2
25
30
35
40
45
50
55
60
65
ξ

Fig. 3

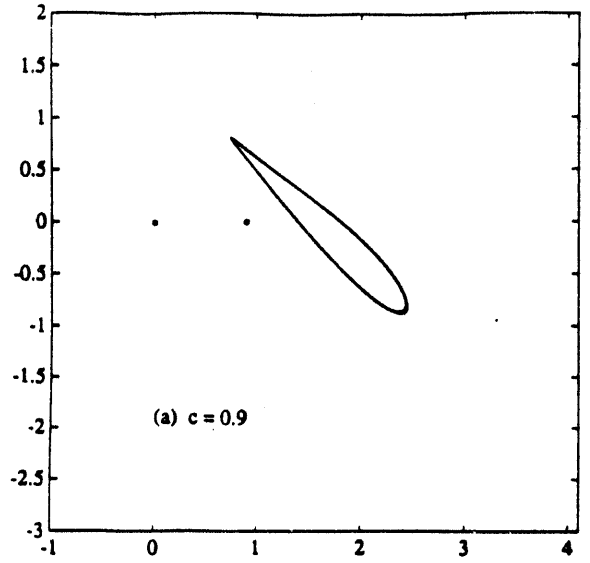

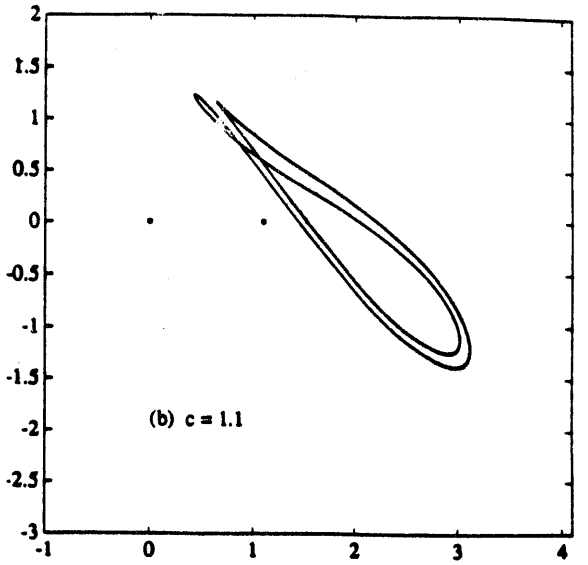

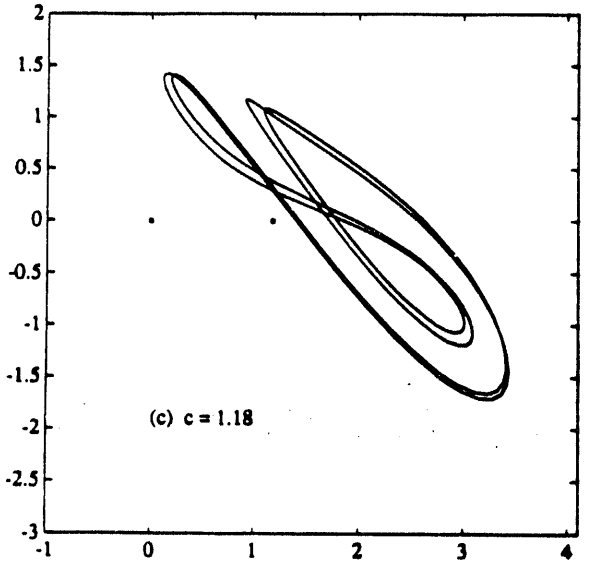

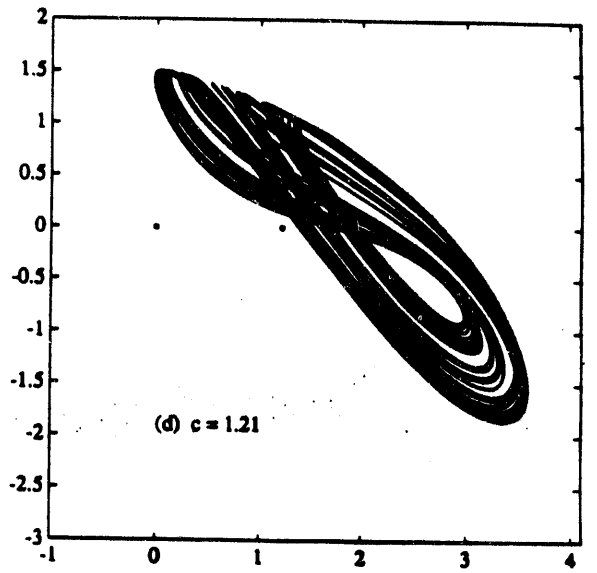

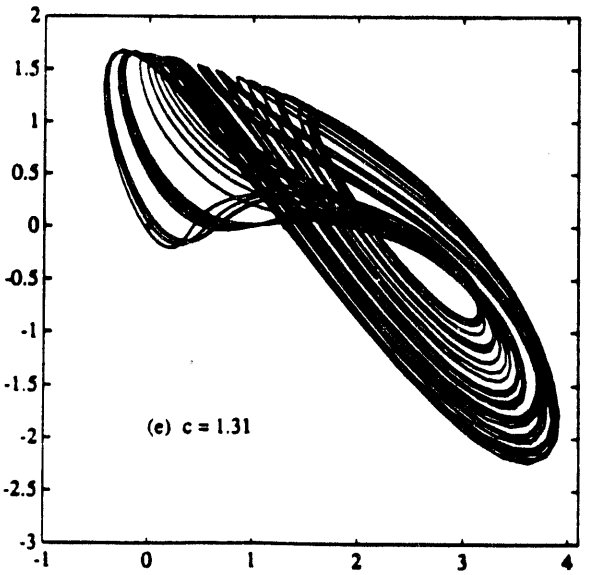

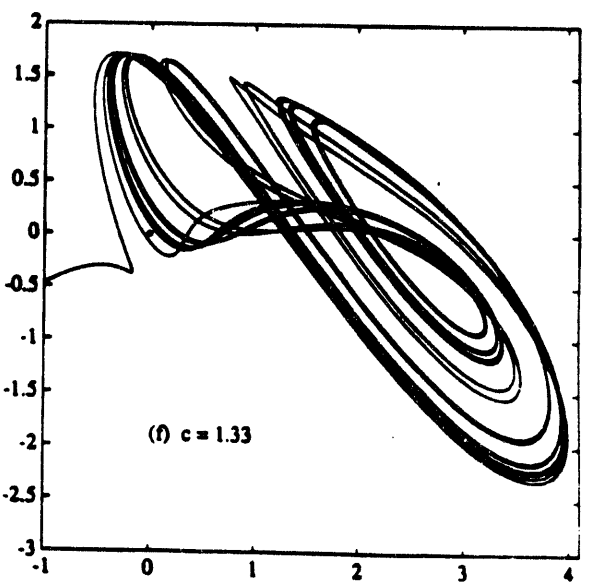

Fig

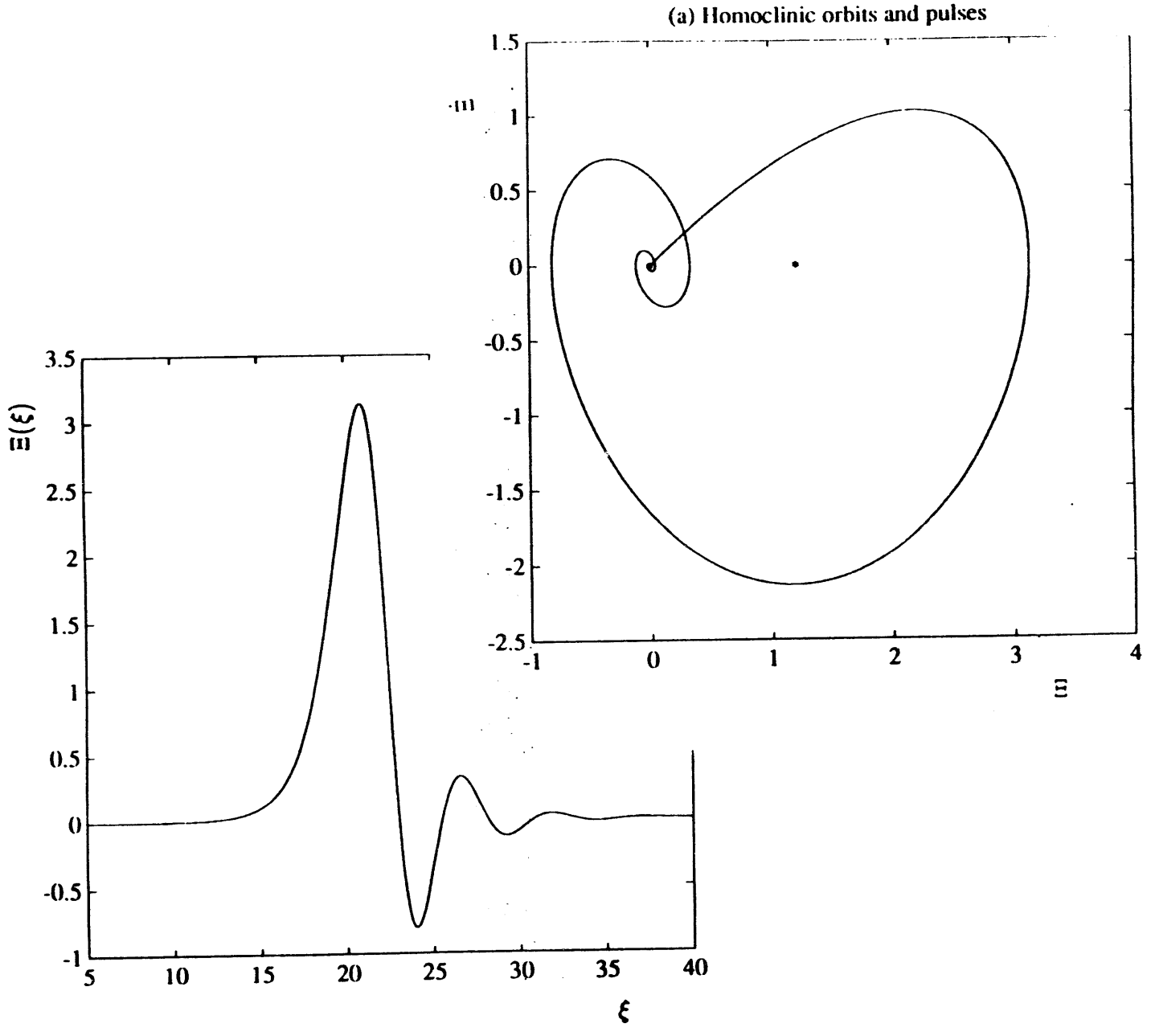

Fig 5(a)

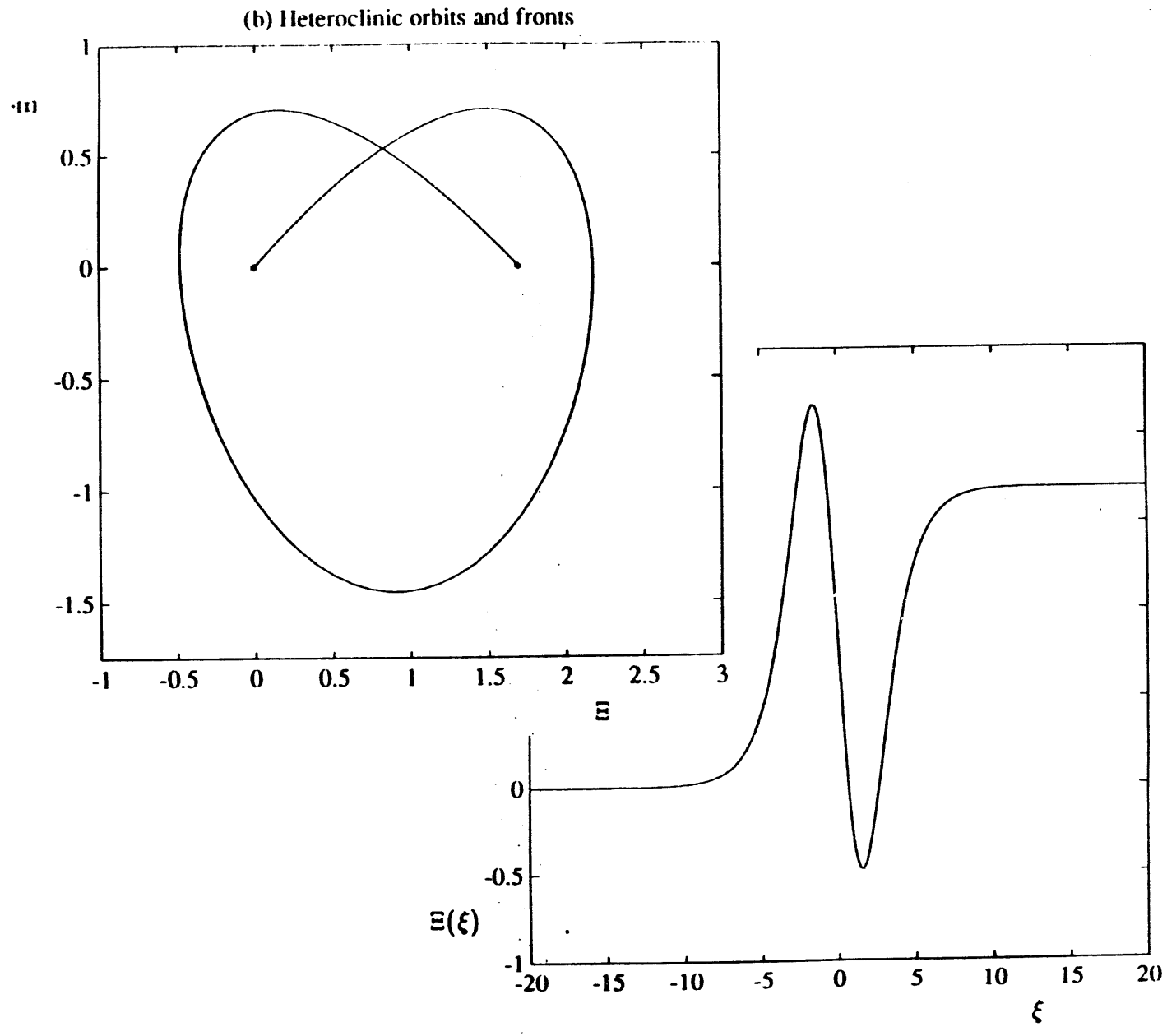
(b) Heteroclinic orbits and fronts
1
0.5
0
-0.5
-1
-1.5
-1
-0.5
0
0.5
1
1.5
2
2.5
3
Ξ
0
-0.5
-1
Ξ(ξ)
-20
-15
-10
-5
0
5
10
15
20
ξ

Fig 5(b)

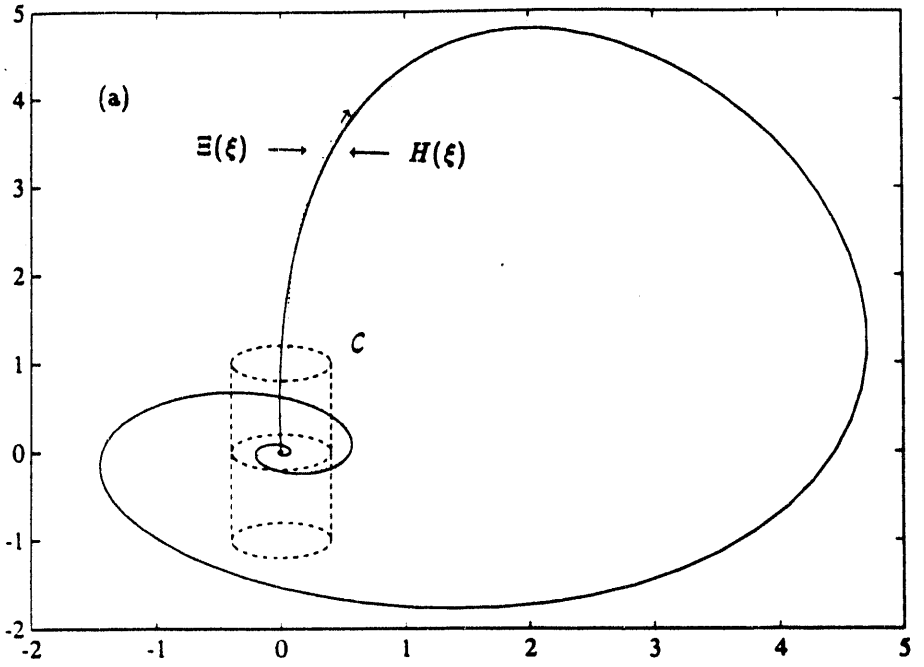

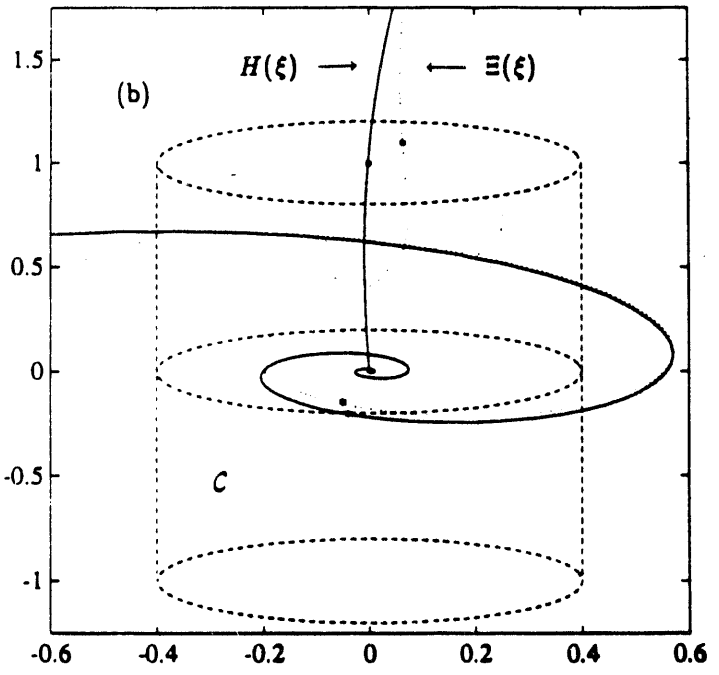

(c) Time series

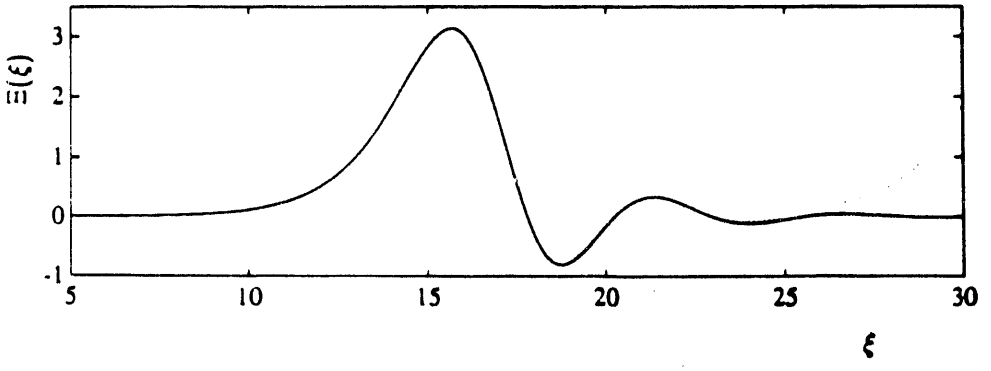

Fig. 6

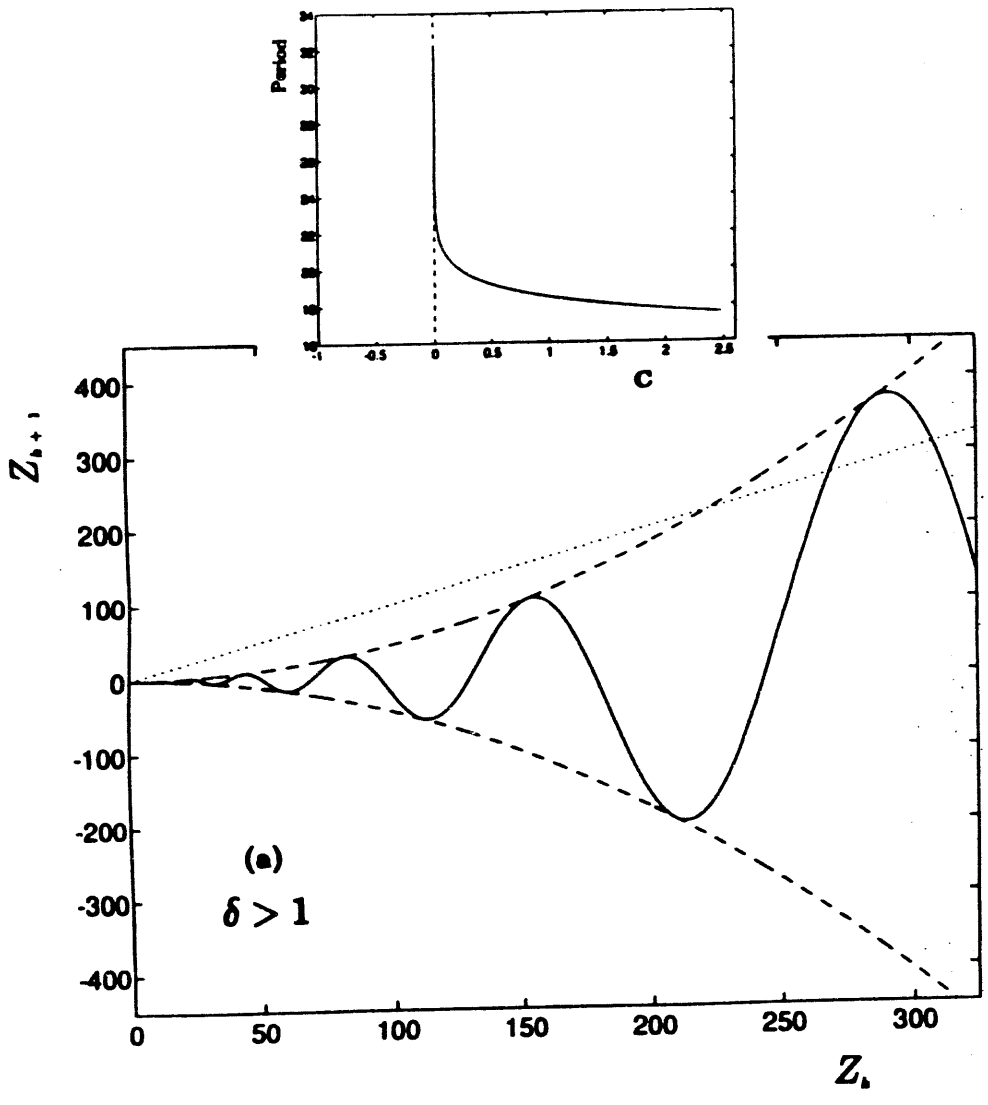
Period
c
Z_{k+1}
400
300
200
100
0
-100
-200
-300
-400
0
50
100
150
200
250
300
Z_k
(a)
$\delta > 1$

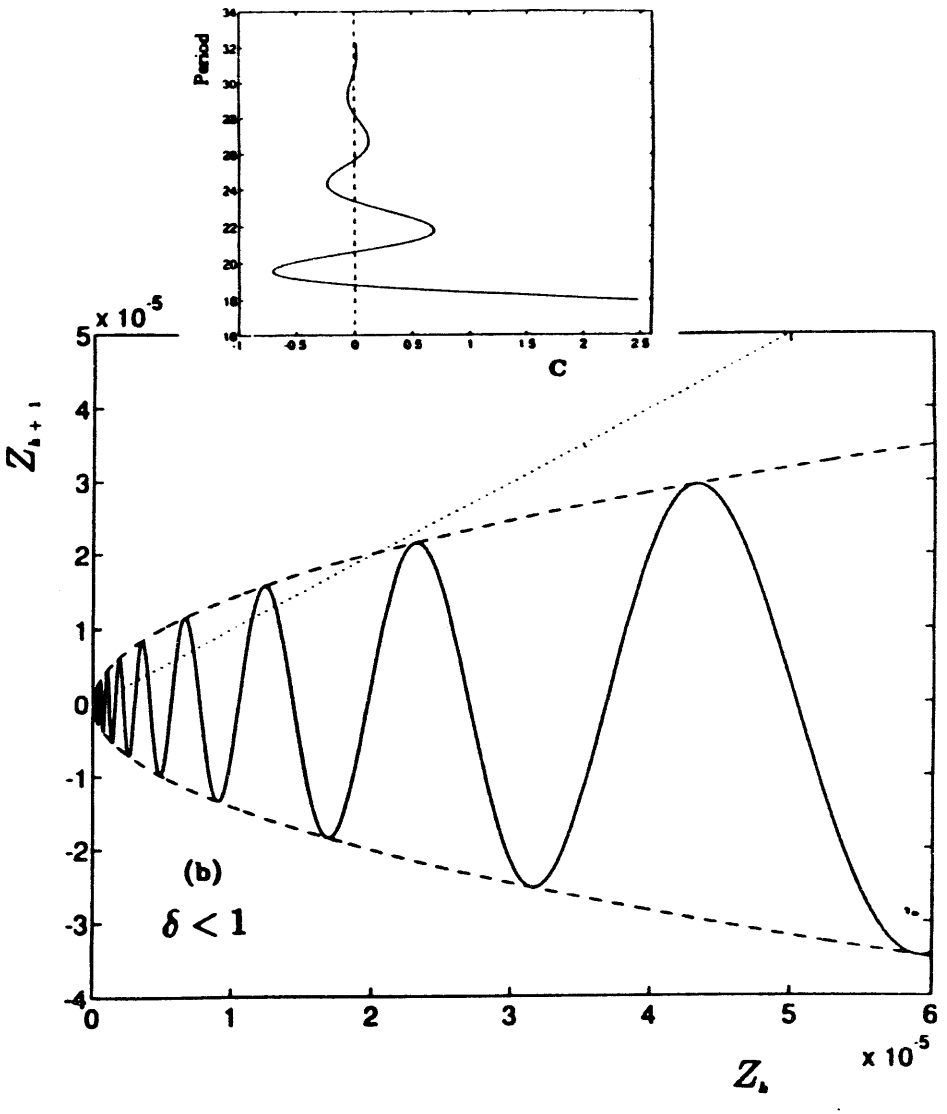
Period
c
x 10^{-5}
Z_{k+1}
5
4
3
2
1
0
-1
-2
-3
-4
0
1
2
3
4
5
6
x 10^{-5}
Z_k
(b)
$\delta < 1$

Fig 7.

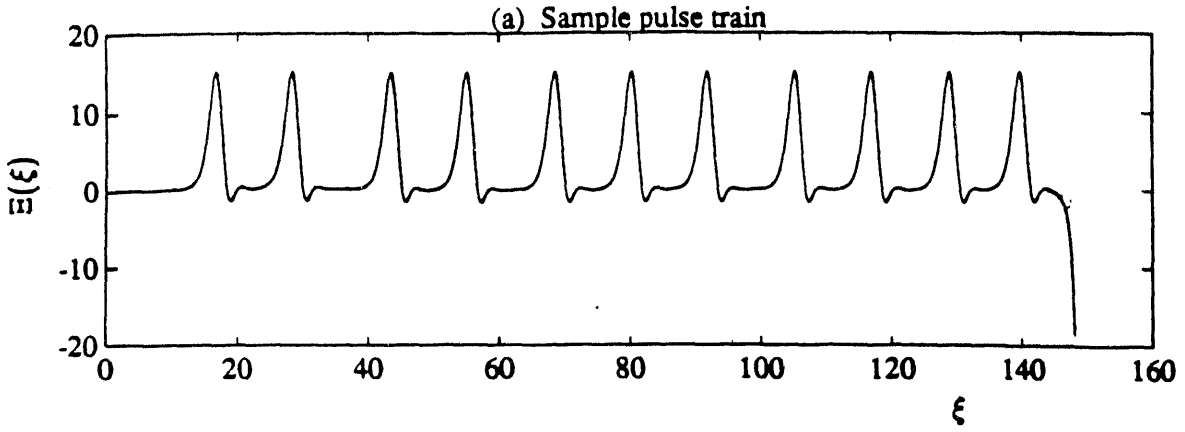
(a) Sample pulse train
20
10
0
-10
-20
0
20
40
60
80
100
120
140
160
Ξ(ξ)
ξ

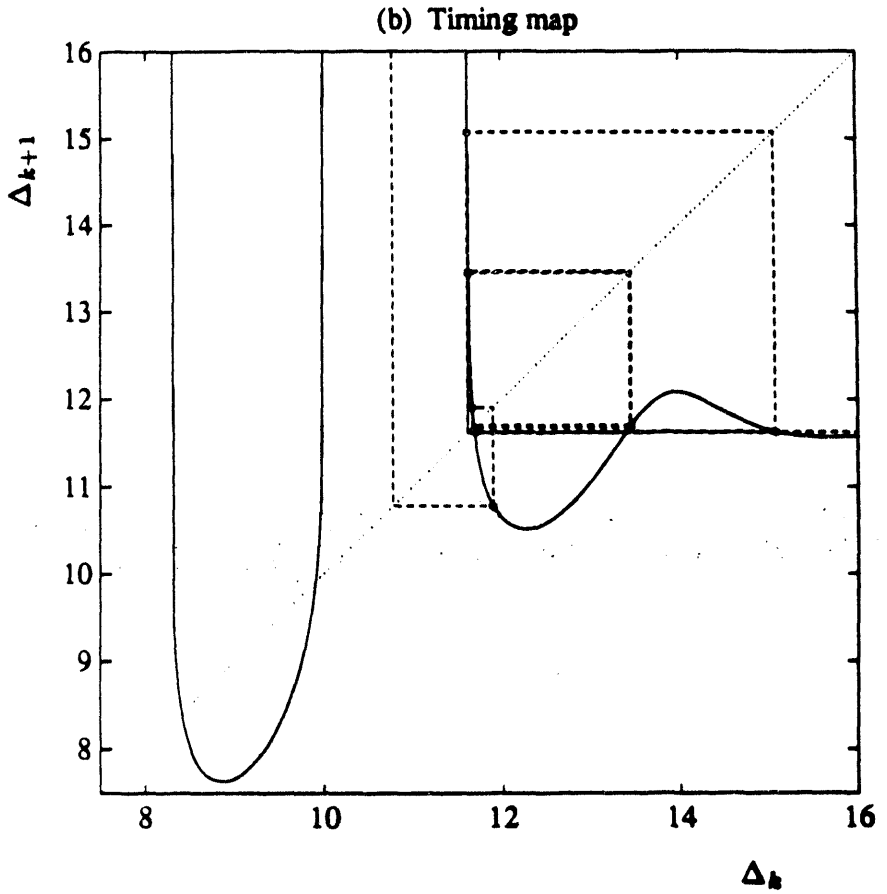
(b) Timing map
16
15
14
13
12
11
10
9
8
8
10
12
14
16
Δk+1
Δk

Fig. 8

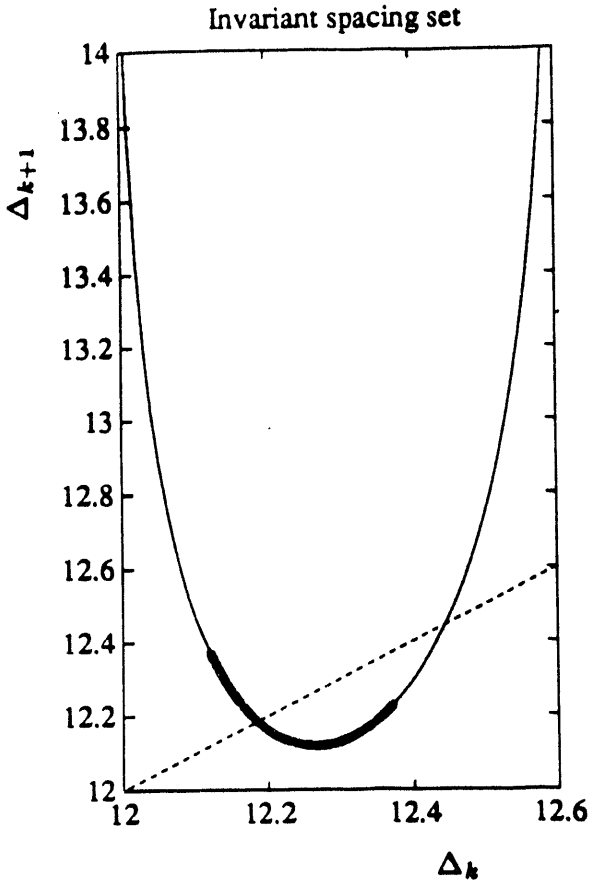
Invariant spacing set
14
13.8
13.6
13.4
13.2
13
12.8
12.6
12.4
12.2
12
12
12.2
12.4
12.6
Δ_{k+1}
Δ_k

Fig. 9

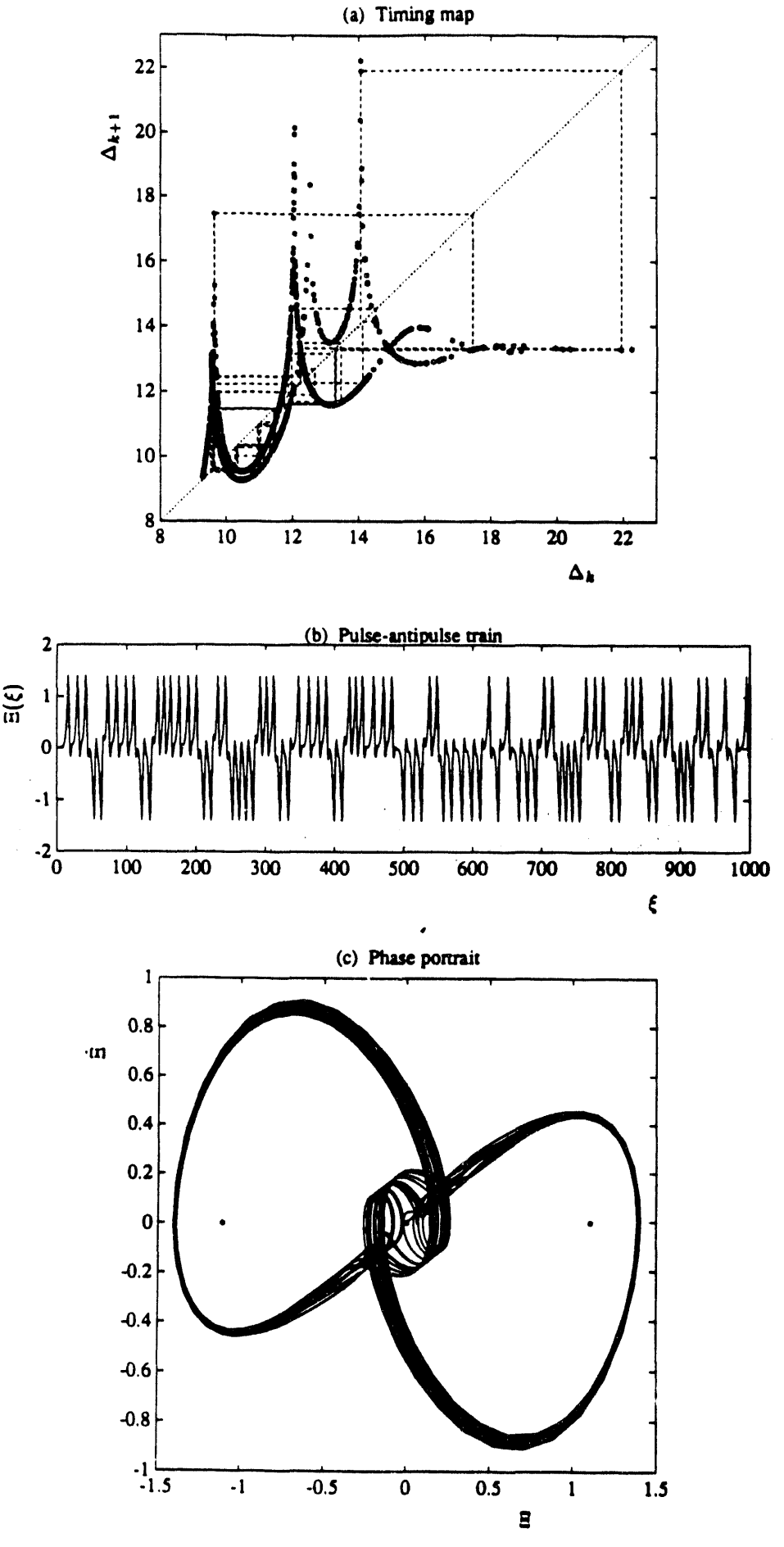
(a) Timing map
Δ_{k+1}
Δ_k
(b) Pulse-antipulse train
$\Xi(\xi)$
ξ
(c) Phase portrait
Ξ

Fig. 10

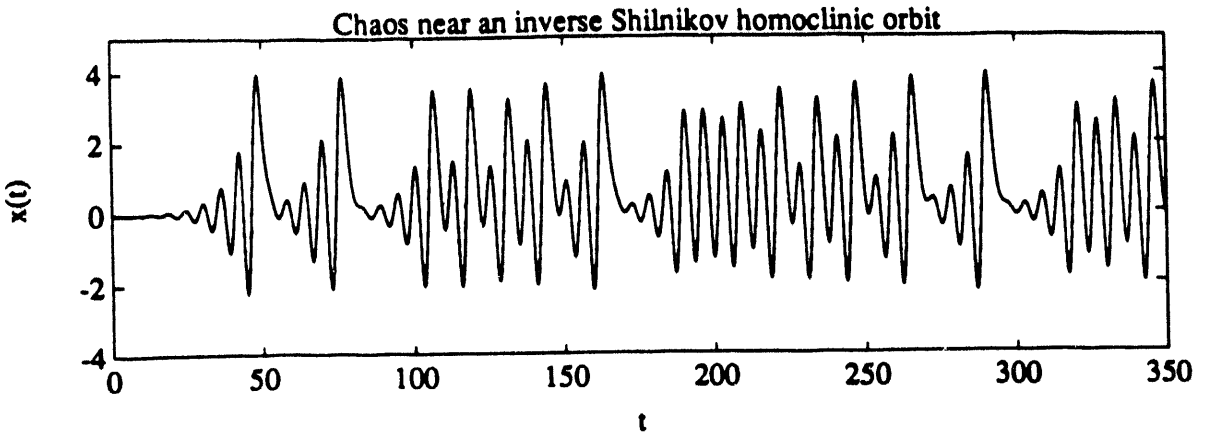
Chaos near an inverse Shilnikov homoclinic orbit
x(t)
4
2
0
-2
-4
0
50
100
150
200
250
300
350
t

Fig. 11

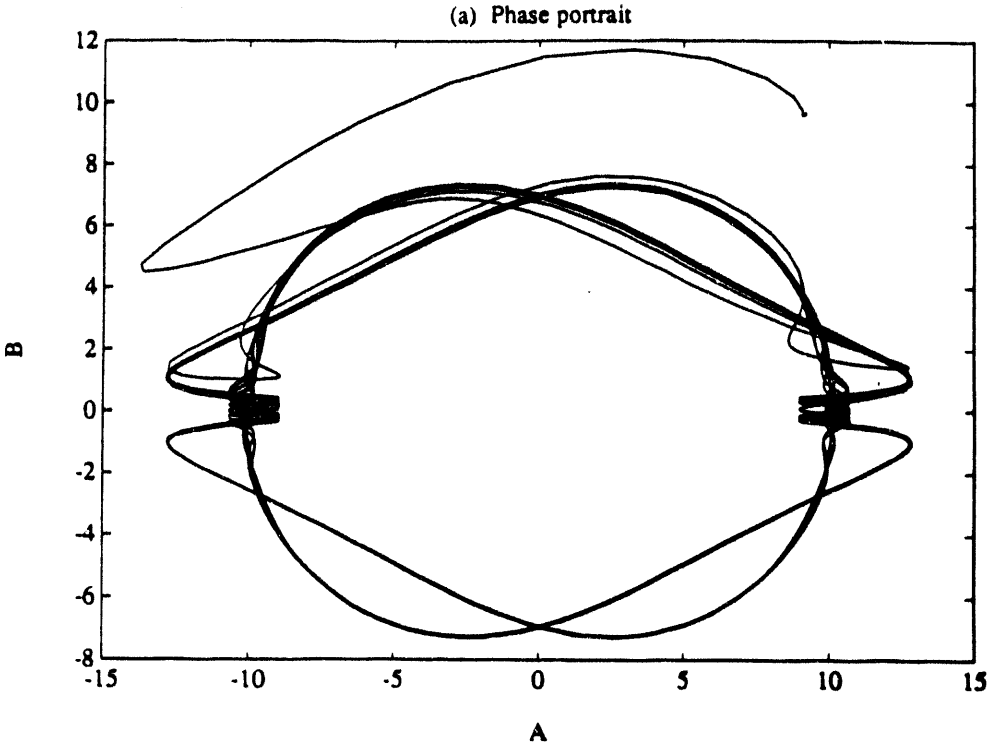
(a) Phase portrait
B
A

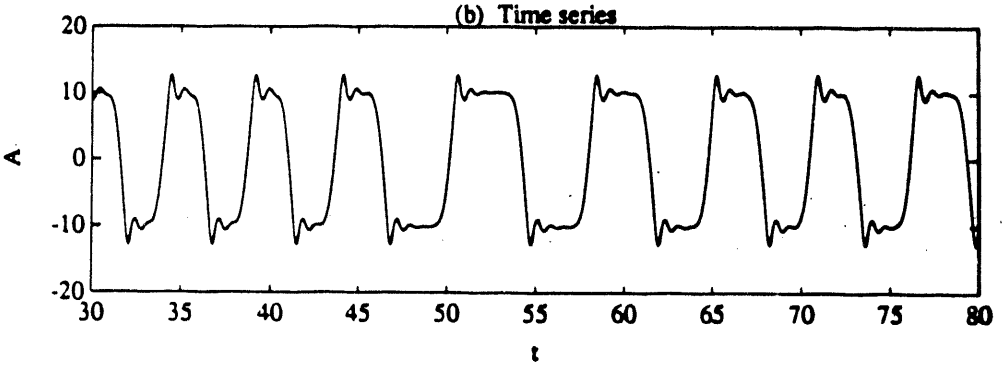
(b) Time series
A
t

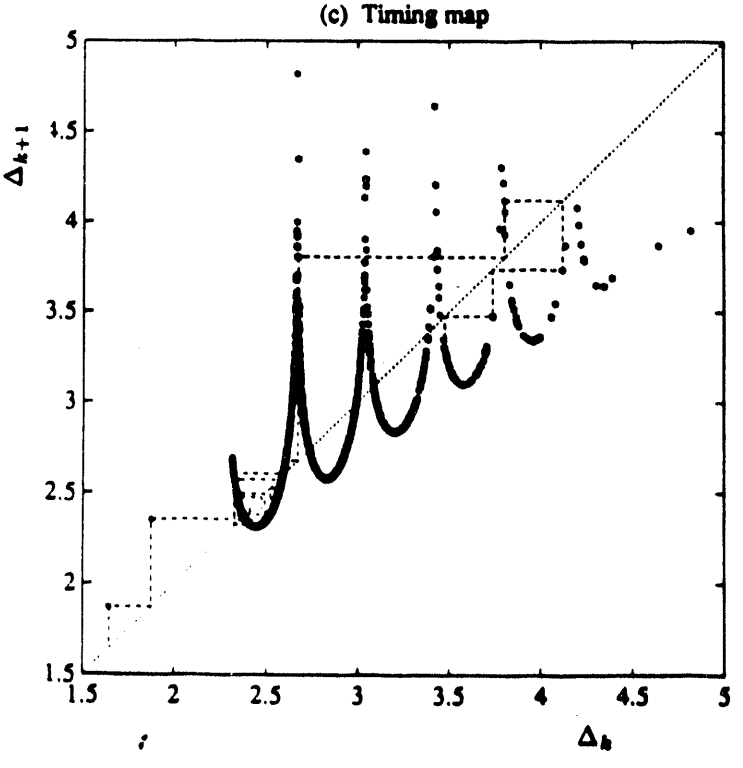
(c) Timing map
Δ_{k+1}
Δ_k

Fig. 12

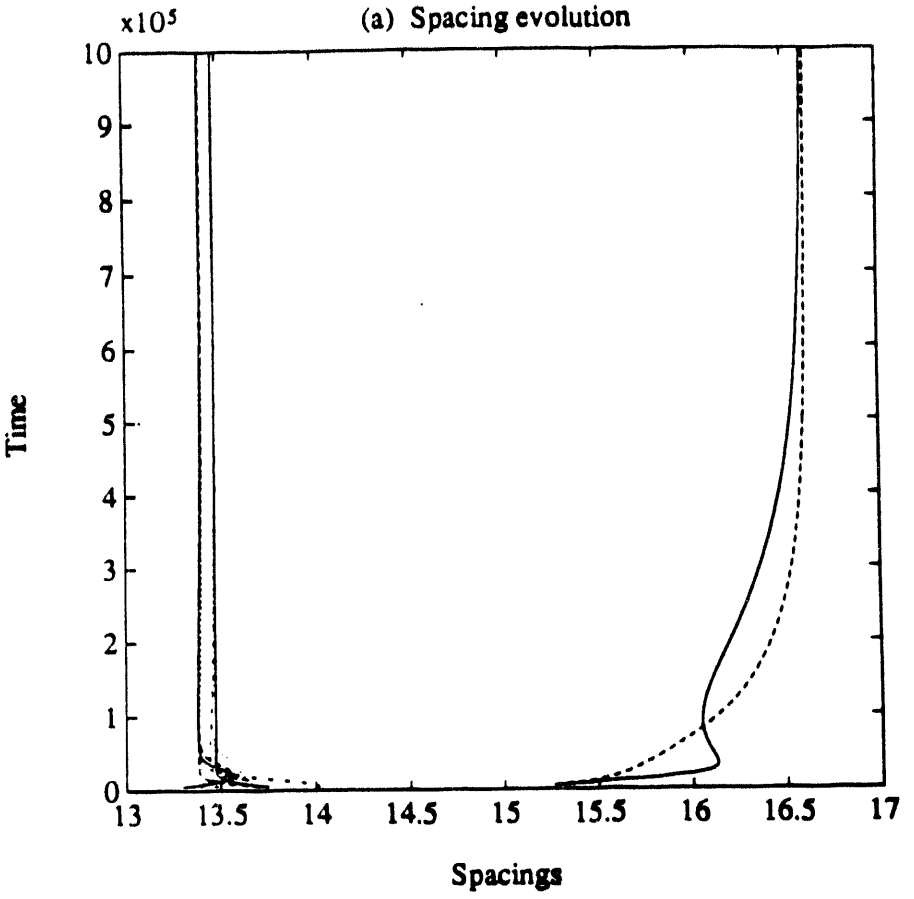
(a) Spacing evolution
x10^5
Time
Spacings
0
1
2
3
4
5
6
7
8
9
10
13
13.5
14
14.5
15
15.5
16
16.5
17

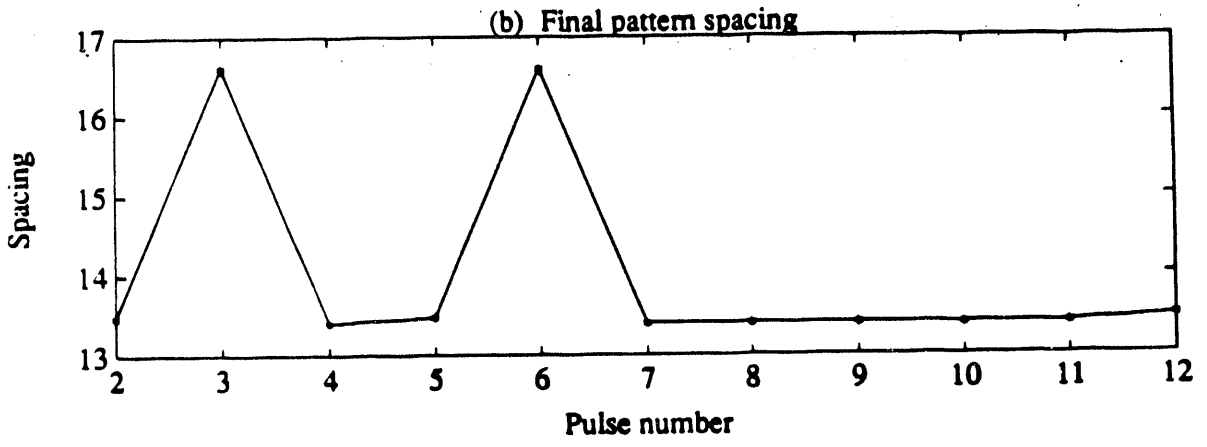
(b) Final pattern spacing
Spacing
Pulse number
13
14
15
16
17
2
3
4
5
6
7
8
9
10
11
12

Fig. 13

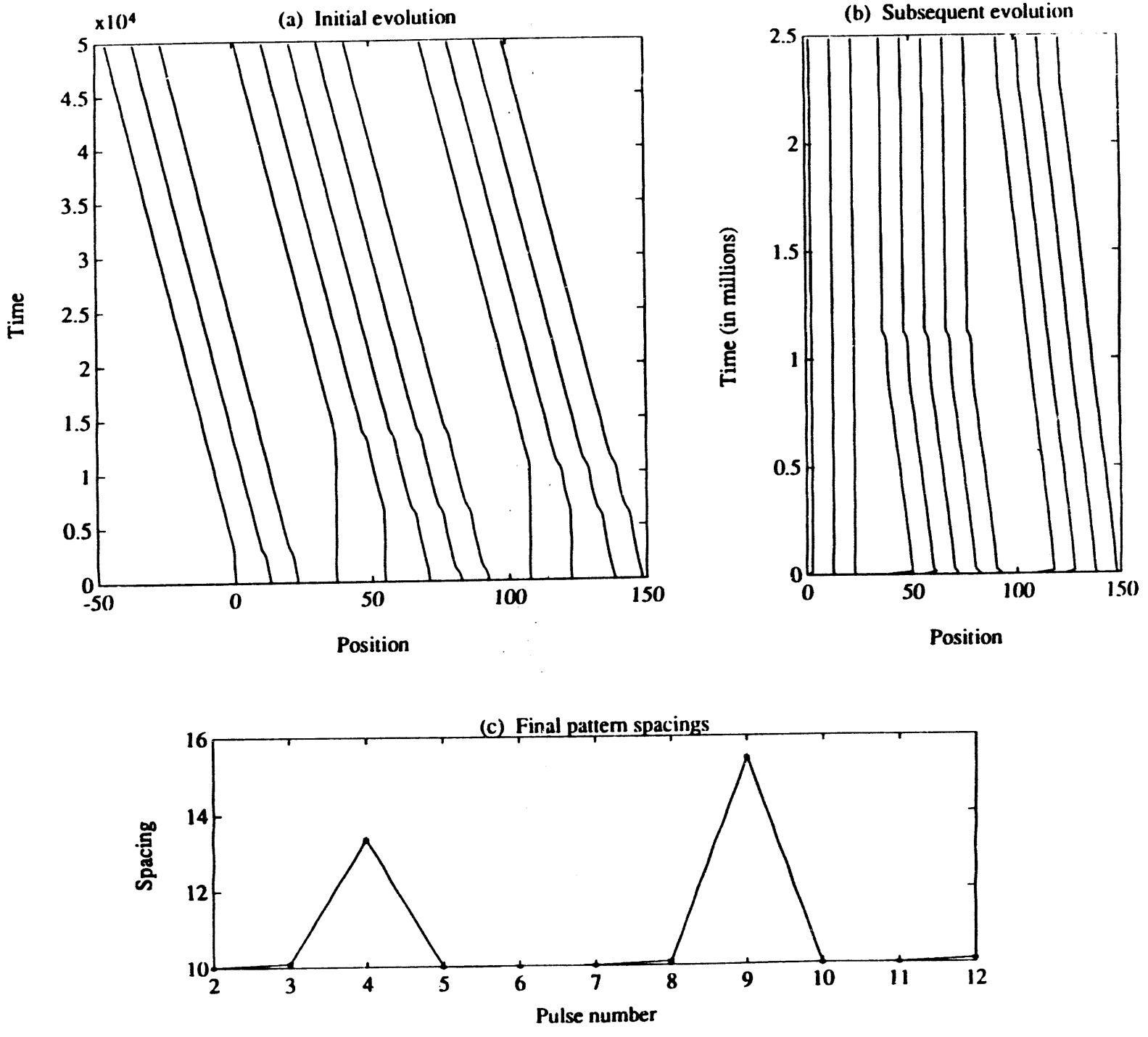
(a) Initial evolution
x10^4
Time
Position
(b) Subsequent evolution
Time (in millions)
Position
(c) Final pattern spacings
Spacing
Pulse number

Fig. 14

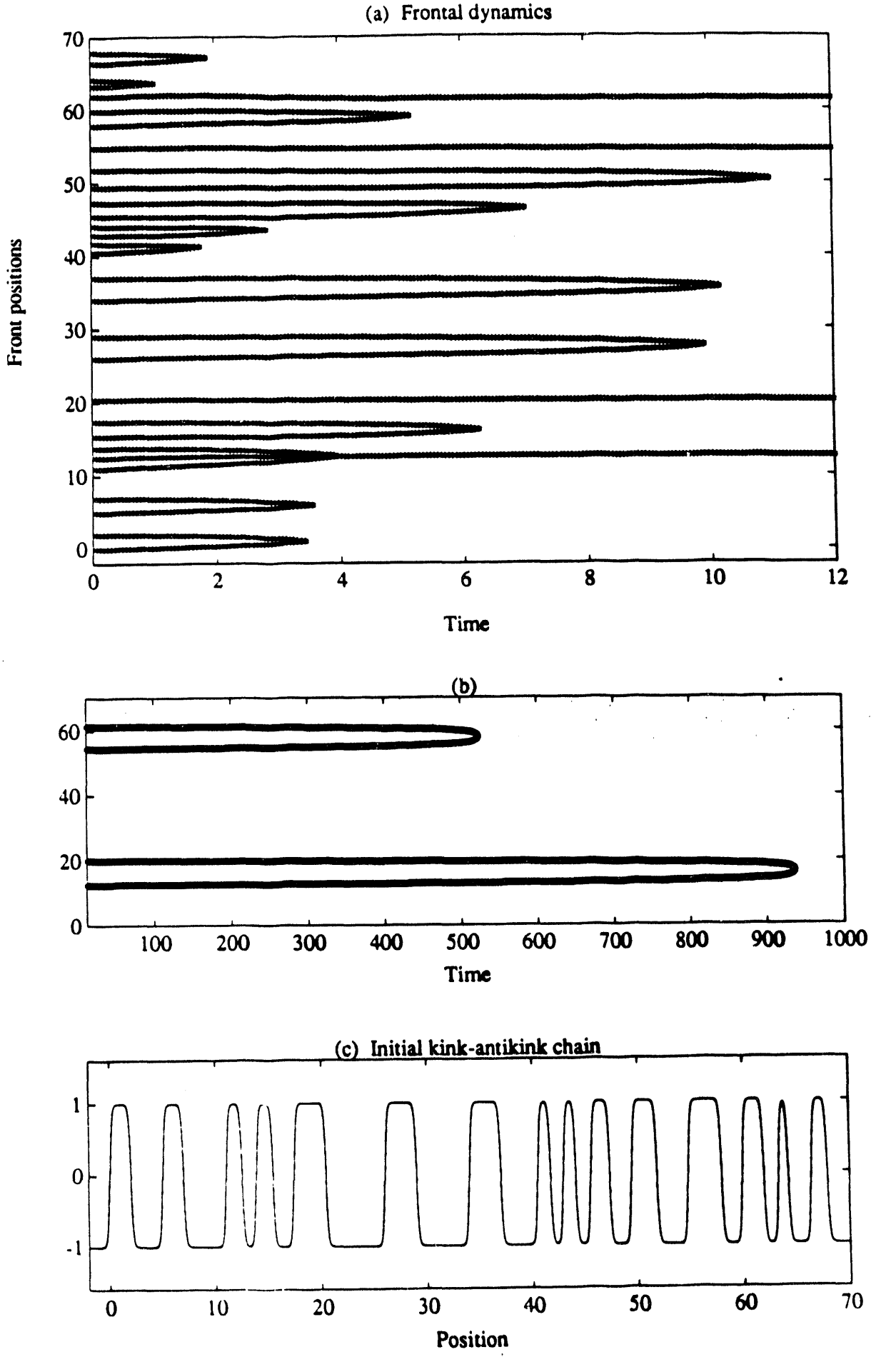
(a) Frontal dynamics
Front positions
Time
(b)
Time
(c) Initial kink-antikink chain
Position

Fig.

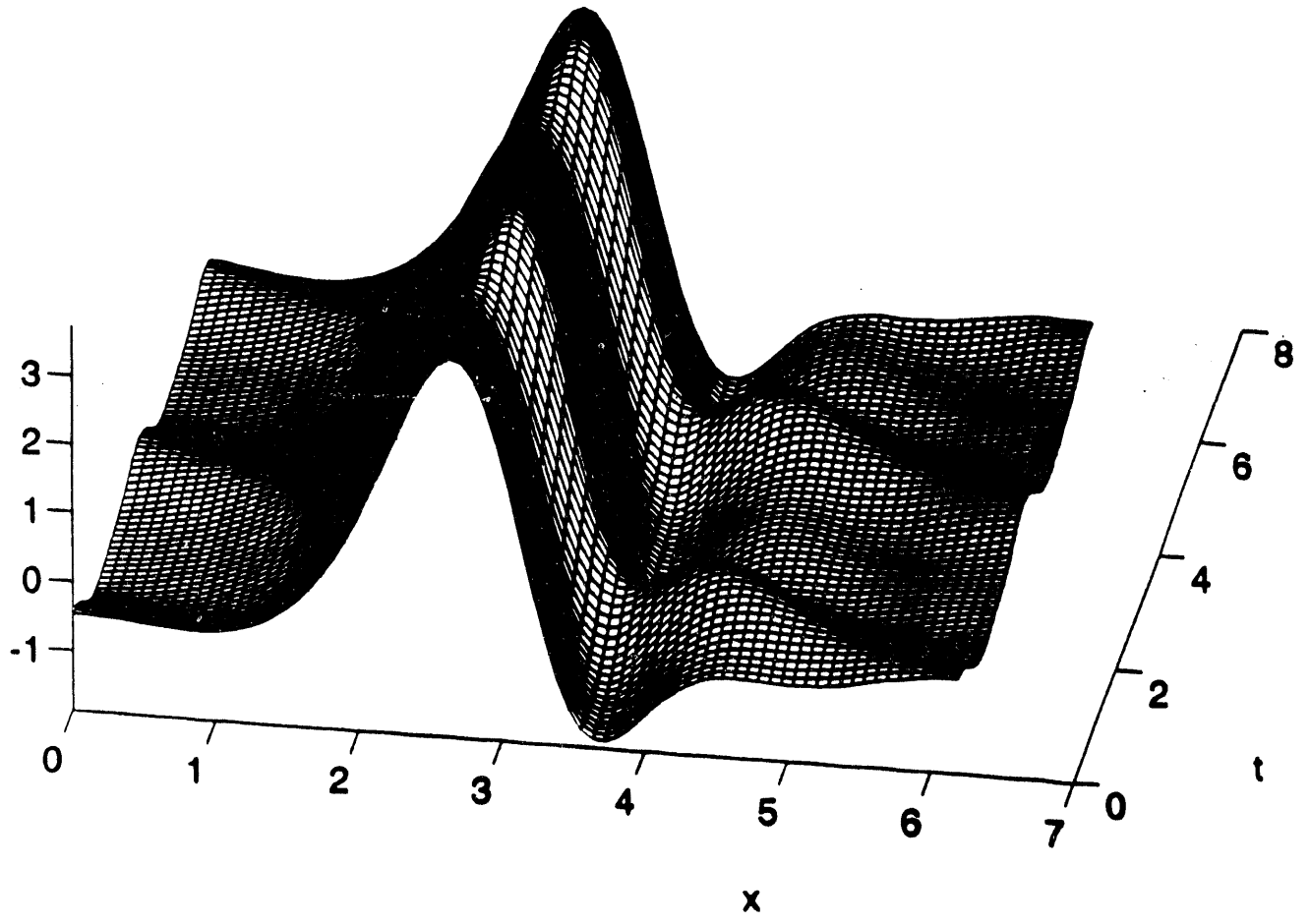

Fig 16.

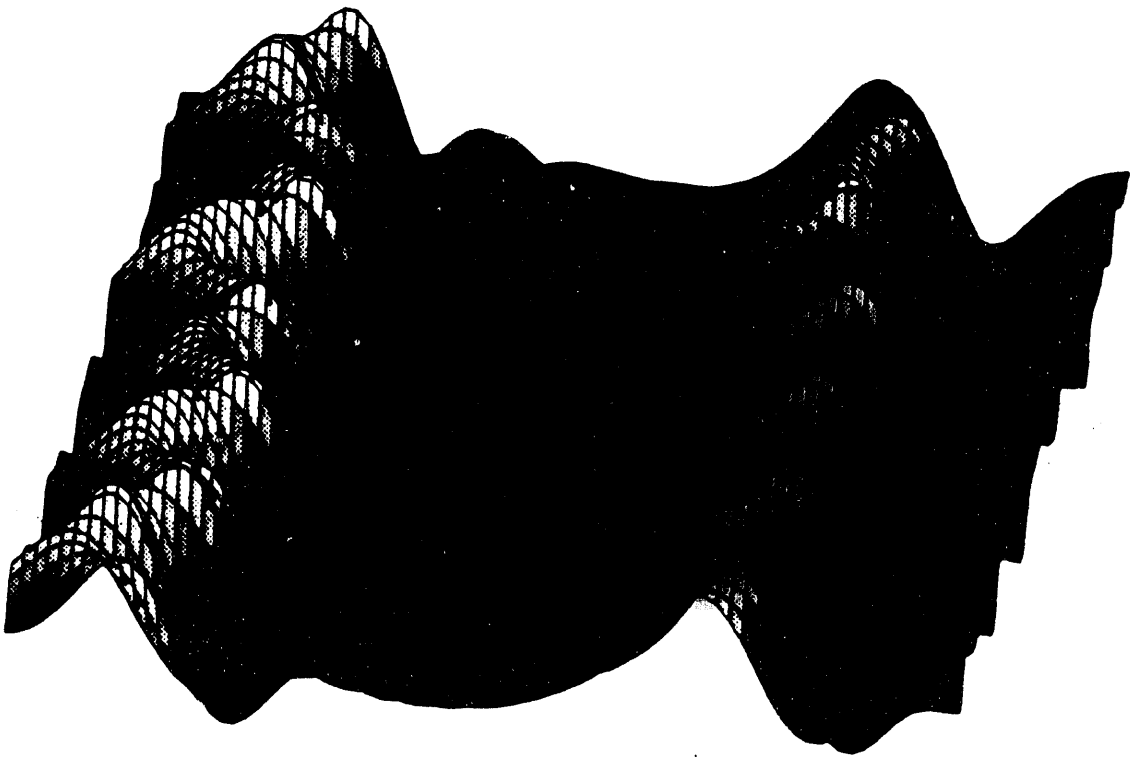

Fig. 17

END

DATE
FILMED
5/16/94